The stochastic movements of individual streambed grains

by

J. Kevin Pierce

B.S. Physics, West Virginia University 2013

M.Sc. Physics, University of British Columbia 2016

A THESIS SUBMITTED IN PARTIAL FULFILLMENT
OF THE REQUIREMENTS FOR THE DEGREE OF

Doctor of Philosophy

in

THE FACULTY OF ARTS
(Department of Geography)

The University of British Columbia
(Vancouver)

June 2021

The following individuals certify that they have read, and recommend to the Faculty of Graduate and Postdoctoral Studies for acceptance, the thesis entitled:

The stochastic movements of individual streambed grains

submitted by **J. Kevin Pierce** in partial fulfillment of the requirements for the degree of **Doctor of Philosophy** in **Department of Geography**.

Examining Committee:

Marwan Hassan, Geography
Supervisor

Brett Eaton, Geography
Supervisory Committee Member

Rui Ferreira, University of Lisbon
Civil Engineering

Magnus Monolith, Other Department
External Examiner

Additional Supervisory Committee Members:

Person1
Supervisory Committee Member

Person 2
Supervisory Committee Member

Abstract

Write an abstract.

Lay Summary

The lay or public summary explains the key goals and contributions of the research/ scholarly work in terms that can be understood by the general public. It must not exceed 150 words in length.

Preface

A preface should be written indicating what is to come and what the point of this whole thing is.

Contents

List of Tables

List of Figures

Acknowledgments

Thanks Leo Golubovic, Mindy Saunders, Calisa and Jim Pierce, Kim and Kelsey Pierce, Johnathan Ramey, Linda Mendez, Tex Wood, Charles Wood, and all of the Appalachian intelligensia who paved my way. Tyler cannon. . .

Shawn Chartrand, Conor McDowell, Matteo Saletti, Will Booker, David Adams, Leo King, Tobias Mueller, Nisreen Ghazi,

Adam Payne, Adam Collins, Megat Denney, Andrew Rice, Evan Graber, Scott Ferris, Craig Tenney, and the rest of the WVU physics lounge family.

Andy Osadetz, Josh Plankeel,

My partner Mary for putting up with the late nights.

Chapter 1

Sediment transport and landscape evolution

Landscapes evolve across geologial time due to energy and mass contributed from above and below the Earth's surface.

1.1 Stochastic properties of sediment movement

1.2 Historical survey: statistical physics in sediment transport

1.3 Philosophy of the statistical physics approach

1.4 What's left?

Chapter 2

Calculation of the sediment flux

2.1 Introduction

A relativity weak flow shearing a bed of sediment entrains individual particles into a state of motion controlled by turbulent forcing and intermittent collisions with other grains at rest on the bed, generating wide fluctuations in the sediment velocity (*Fathel et al.*, 2015; *Heyman et al.*, 2016). Bed load particles move downstream until they are disentrained when they happen to encounter sufficiently sheltered divots on the bed surface to interrupt their motions (*Charru et al.*, 2004; *Gordon et al.*, 1972). Eventually, the bed around them rearranges and destroys this shelter, or turbulent fluctuations overcome the shelter (**??**), particles are once again entrained, and the cycle repeats. Bed load transport is thus a kind of itinerant motion, characterized by alternation between fluctuating movements and rest. This process has proven itself extremely challenging to describe mathematically, given the technicality of the stochastic physics required (**??**).

To date, descriptions of bed load transport have therefore simplified the problem in various ways to enable progress. The foundational work is due to Einstein, who considering bed load motions as instantaneous, so he could describe bed load transport as an alternating sequence of "steps" and rests having random length and duration (*Einstein*, 1937), in a pioneering application of the continuous time random walk (*Montroll*, 1964). Einstein concluded that particles move downstream with a mean velocity $\langle u \rangle = k_E l$, where k_E is the rate at which an individual bed

particle entrains into motion, and l is the mean length of each downstream step. Later, he applied these ideas to calculate the mean downstream flux of many particles (*Einstein*, 1950). Einstein reasoned that if the density of resting particles on the bed is ρ_b, the overall areal entrainment rate of particles can be written $E = \rho_b k_E$, so the mean downstream sediment flux can be expressed as $\langle q_s \rangle = \rho_b \langle u \rangle = El$.

Many researchers have since refined Einstein's approach to provide more realistic descriptions of individual particle motions than Einstein's instantaneous step model. One set of efforts has concentrated on particle motions only, calculating the downstream velocity distributions of moving particles using Langevin-type equations to describe turbulent flow and collision forces (**???**). These models do not yet include transitions between motion and rest. Another set of efforts has concentrated on including both motion and rest phases while promoting Einstein's instantaneous steps into finite periods of motion (*Lajeunesse et al.*, 2018; *Lisle et al.*, 1998; **?**), but due to mathematical challenges, these models characterize particle motions by a constant velocity, rather than the fluctuating velocities that real sediment particles exhibit.

Researchers have also refined stochastic formulations of the sediment flux beyond the description of the mean flux provided by Einstein (*Furbish et al.*, 2012a). Experiments demonstrate that the sediment flux exhibits wide fluctuations due to (1) variations in the number of moving particles and (2) variations in the velocities of moving particles (*Ancey et al.*, 2008; **?**). As a result of these sediment tranport fluctuations, measurements of the mean sediment flux depend on the timescale over which they are collected (*Singh et al.*, 2009; **?**; **?**), giving a scale-dependent character to the mean sediment flux. To date, very few models have calculated the probability distribution of the bed load sediment flux, and among these, even fewer have described any observation-scale dependence of the sediment flux (**?**).

This survey reveals two major issues in need of research attention. First, we do not yet have the capability to describe individual sediment trajectories through motion and rest including velocity fluctuations in the motion state; and second, we need more understanding of how to connect individual particle trajectories through motion and rest to the overall downstream sediment flux probability distribution and the dependence of the moments of this distribution on the observation time. Here, we develop a new statistical physics-based formalism which addresses both

of these problems by describing individual particle trajectories with a Langevin-type equation of motion. This stochastic equation includes alternation between motion and rest at random intervals, and the motion state includes stochastic forcing that ascribes fluctuating velocities to moving particles. Using the probability distribution of particle position generated by this model, we construct a formalism to derive analytically the probability distribution of the sediment flux, and this distribution includes an explicit observation-scale dependence. Below, we develop the new formalism in sec. 2.2, solve it in sec. 2.4, and we discuss the implications of our results and future research ideas in secs. 2.5 and 2.6.

2.2 Model development

We consider an infinite one-dimensional domain populated with sediment particles on the surface of a sedimentary bed. We consider that the flow is weak enough that interactions among moving grains are very rare, although interactions between moving particles and the bed may be common. The flow is in constrast strong enough so that particles are in motion. We label the downstream coordinate as x, so that the downstream velocity of a moving particle is $\dot{x}$, and we describe all sediment particles as independent from one another, but governed by the same underlying dynamical equations, meaning we neglect any influence of sediment size or shape or spatial variations in the overlying fluid flow.

2.2.1 Dynamical equation for bed load sediment transport

From these assumptions, our first target is to write an equation of motion for the individual sediment particle encompassing two features. First, particles should alternate between motion and rest. The transition rate from rest to motion is called entrainment and occurs with probability per unit time (or rate) k_E, while the transition from motion to rest is called deposition and occurs with rate k_D. Second, particles in motion should move with mean velocity V and some fluctuations around this velocity. The simplest equation of motion including these features is

$$\dot{x}(t) = [V + \sqrt{2D}\xi(t)]\eta(t). \tag{2.1}$$

Here $\xi(t)$ is a Gaussian white noise having zero mean and unit variance representing velocity fluctuations among moving particles, and $\eta(t)$ is a dichotomous noise which takes on values $\eta = 1$, representing motion, and $\eta = 0$, representing rest. Here, V is the mean particle velocity, and D is a diffusivity [units L^2/T] of moving particles. The transition rate from $\eta = 0$ to $\eta = 1$ is k_E, and the transition rate from $\eta = 1$ to $\eta = 0$ is k_D. We write $k = k_E + k_D$ as a shorthand.

2.2.2 Derivation of the master equation for $P(x,t)$

The solution of equation 2.1 for a given realization of the two noises $\eta(t)$ and $\xi(t)$ gives the trajectory of a single particle. Averaging over the ensemble of all such trajectories from different realizations of the noises will obtain the probability distribution $P(x,t)$ that a particle which started at position $x = 0$ at time $t = 0$ has travelled to position x by time t. This distribution, by construction, will generalize earlier models which did not include velocity fluctuations among moving particles (*Lajeunesse et al.*, 2018; *Lisle et al.*, 1998).

We form the desired probability distribution of position as $P(y,t) = \left\langle \delta(y - x(t)) \right\rangle_{\eta,\xi}$, where $x(t)$ is the formal solution of eq. 2.1 and the average is over both noises, but this symbolic equation is not yet useful as taking these averages directly is a challenging mathematical problem (**?**). A simpler approach is to conduct the necessary averages in Fourier space. Integrating eq. 1, using its solution in the probability distribution, then Fourier transforming gives

$$\tilde{P}(g,t) = \left\langle \left\langle \exp\left[-ig \int_0^t du[V + \sqrt{2D}\xi(u)]\eta(u) \right] \right\rangle_\eta \right\rangle_\xi . \tag{2.2}$$

Taking time derivatives and conducting the averages using known characteristics of averages of exponentials of Gaussian white noise (*Gardiner*, 1983; **?**) and the Furutsu-Norikov procedure for time derivatives of averages involving dichotomous noise (**?**), in a method similar to (**?**), provides the Fourier-space master equation

$$\partial_t^2 \tilde{P}(g,t) = (igV - g^2 D - k)\partial_t \tilde{P} + k_E(igV - g^2 D)\tilde{P}, \tag{2.3}$$

and inverse Fourier transforming provides the master equation

$$(\partial_t^2 + V\partial_x\partial_t + k_E V\partial_x + k\partial_t - D\partial_x^2\partial_t - k_E D\partial_x^2)P(x,t) = 0. \tag{2.4}$$

This is a diffusion-like equation governing the probability distribution of position for individual particles as they transport downstream through a sequence of motions and rests, with the movement velocity being a random variable. One can see in particular that taking an the entrainment rate k_E very large, meaning that all particles are generally moving, implies an advection-diffusion equation $(\partial_t + V\partial_x - D\partial_x^2)P = 0$ for the position, characteristic of a particle moving downstream with Gaussian velocity fluctuations. Otherwise, with k_E of similar order as k_D, there is a finite probability that the particle is at rest, and the advection-diffusion process is often interrupted by deposition, giving rise to the additional terms in eq. 3.7.

2.3 Formalism for the downstream sediment flux

Now we express the probability distribution of the sediment flux using the probability distribution of particle position $P(x,t)$ provided as the solution of equation 3.7. We apply a modified version of the approach recently developed by Banerjee and coworkers for (**?**). The basic idea, as depicted in Figure 1, is that we distribute particles in all states of motion along a domain at random locations at $x < 0$, then we calculate using $P(x,t)$ the rate of particle arrival to $x > 0$ within the sampling time T.

The rate of particles crossing the surface in an observation time T is

$$Q(T) = \frac{1}{T}\sum_{i=1}^{N} \mathscr{I}_i(T). \tag{2.5}$$

In this equation, $\mathscr{I}_i(T)$ is an indicator function which is 1 whenever the ith particle has passed our control surface and 0 otherwise. All particles which have not crossed the control surface (or which have crossed and then crossed back) con-

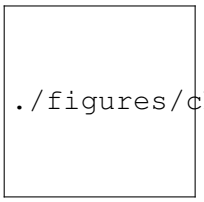

Figure 2.1: The left panel indicates the configuration for the flux. The particle trajectories within are calculated from equation 2.1, demonstrating alternation between rest and motion with fluctuating velocity. Particles begin their transport with positions $-L \leq x \leq 0$ at $t = 0$, and as depicted in the right panel, the flux is calculated as the number of particles $N_>(t)$ which lie to the right of $x = 0$ at the observation time t, divided by t: $Q(t) = t^{-1}N_>(t)$. We calculate the probability distribution of Q over all realizations of the trajectories and initial positions as $L \to \infty$

tribute nothing to the flux. The probability distribution of the flux is then

$$P(Q|T) = \left\langle \delta\Big(Q - \frac{1}{T}\sum_{i=1}^{N} \mathscr{I}_i(T)\Big)\right\rangle. \tag{2.6}$$

The average is over the initial conditions of each particle and the ensemble of trajectories for each particle. Taking the Laplace transform over Q (i.e. forming the characteristic function) obtains

$$\tilde{P}(s|T) = \left\langle \int_0^\infty dQ e^{-sQ}\delta\Big(Q - \frac{1}{T}\sum_{i=1}^{N} \mathscr{I}_i(T)\Big)\right\rangle \tag{2.7}$$

$$= \left\langle \exp\Big(\frac{s}{T}\sum_{i=1}^{N} \mathscr{I}_i(T)\Big)\right\rangle \tag{2.8}$$

$$= \prod_{i=1}^{N}\left\langle \exp\Big(-\frac{s}{T}\mathscr{I}_i(T)\Big)\right\rangle \tag{2.9}$$

$$= \prod_{i=1}^{N}\Big[1 - \big(1 - e^{-s/T}\big)\big\langle \mathscr{I}_i(T)\big\rangle\Big] \tag{2.10}$$

This progression relies on the independence of averages for each particle (so the average of a product is the product of averages) and the fact that $\mathscr{I}_i(T)$ is either 1 or 0 ($e^{ax} = 1 - (1 - e^a)x$ if $x = 0, 1$). The average over initial conditions and

possible trajectories for the ith particle can be written

$$\langle \mathscr{I}_i(t) \rangle = \frac{1}{L}\int_L^0 dx' \int_0^\infty dx \mathscr{P}(x,t|x') = \frac{1}{L}\int_0^L dx' \int_0^\infty dx \mathscr{P}(x,t|-x'), \qquad (2.11)$$

where $\mathscr{P}(x,t|x')$ is the probability density that the particle is found at position x at time t given it was initially at x' at time 0. This is the part of the flux that depends on the particle dynamics (ie instantenous velocities and entrainment/deposition characteristics).

Inserting (7) into (6) and taking the limit as $L \to \infty$ and $N \to \infty$ while the density of particles $\rho = N/L$ remains constant provides

$$\tilde{P}(s|T) = \lim_{N\to\infty} \Big(1 - \frac{1}{N}\big(1 - e^{-s/T}\big)\mu(T)\Big)^N = \exp\Big[-\big(1 - e^{-s/T}\big)\mu(T)\Big]. \quad (2.12)$$

where $\mu(T) = \rho \int_0^\infty dx \int_0^\infty dx' \mathscr{P}(x,T|x')$ is a rate constant which encodes the particle dynamics. This expression is the characteristic function of a Poisson distribution. Expanding in $e^{-s/T}$ and inverting the Laplace transform provides the distribution of the flux

$$P(Q|T) = \sum_{k=0}^{\infty} \frac{\mu(T)^k}{k!} e^{-\mu(T)} \delta(Q - \frac{k}{T}). \qquad (2.13)$$

This equation implies that the mean flux is $\langle Q \rangle(T) = \int_0^\infty dQ Q P(Q|T) = \mu(T)/T$, and similarly the variance is $\sigma_Q^2(T) = \mu(T)/T^2$. The conclusion is that if the flux is considered as a time averaged number of particles crossing a control surface, the mean flux is always Poissonian no matter how particles move, provided they do not interact with one another.

2.4 Results

2.4.1 Derivation of the position probability distribution and its moments

$$P(x,0) = \delta(x) \qquad (2.14)$$

$$\partial_t P(x,0) = -\frac{V k_E}{k} \delta'(x) \qquad (2.15)$$

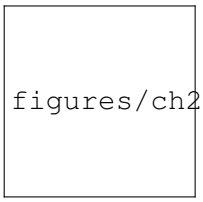

Figure 2.2: The left panel shows the probability distribution of position evolving through time. From the initial state, which is a mixture of moving and resting particles, the distribution splits at short times into contributions from Delta function-like stationary particles and Normal-like moving particles. The right panel demonstrates the resulting spreading characteristics of particles. This short-time splitting noted in the left panel gives rise to ballistic diffusion at short timescales, followed by normal diffusion, as exemplified by equation 4.8.

These initial conditions come from the initial state

$$P(x,0) = \lim_{t\to 0} \frac{k_E}{k}\delta(x-Vt) + \frac{k_D}{k}\delta(x). \tag{2.16}$$

$$\tilde{\tilde{P}}(g,s) = \frac{s+k+Dg^2 - igVk_D/k}{s(s+k)+(Dg^2-igV)(s+k_E)}. \tag{2.17}$$

$$\tilde{P}(x,s) = \frac{-D\partial_x^2 + Vk_D/k\partial_x + s + k}{VR(s+k_E)} \exp\Big[\frac{Vx}{2D} - \frac{V|x|}{2D}R\Big]. \tag{2.18}$$

$$R = \sqrt{1+\frac{4D}{V^2}\frac{s(s+k)}{s+k_E}} \tag{2.19}$$

$$P(x,t) = \big[-D\partial_x^2 + Vk_D/k\partial_x + k + \delta(t) + \partial_t\big]\int_0^t \mathscr{I}_0\Big(2\sqrt{k_E k_D u(t-u)}\Big)e^{-k_E(t-u)} \times \sqrt{\frac{1}{4\pi Du}}\exp\Big[-k_D u - \frac{(x-Vu)^2}{4Du}\Big]du \tag{2.20}$$

The mean is $\langle x\rangle = k_E Vt/k$. The variance is

$$\sigma_x^2 = 2\Big[\frac{k_E V^2 k_D}{k^3} + \frac{k_E D}{k}\Big]\Big(\frac{1}{k}e^{-kt} - \frac{1}{k} + t\Big) \tag{2.21}$$

2.4.2 Calculation of the flux

$$\mu(t) = \rho \int_0^\infty dx_i \int_0^\infty dx P(x + x_i, t). \tag{2.22}$$

Taking the Laplace transform,

$$\tilde{\mu}(s) = \rho \int_0^\infty dx_i \int_0^\infty dx \tilde{P}(x + x_i, s). \tag{2.23}$$

$$\mu(t) = \rho \int_0^t \mathscr{I}_0\left(2\sqrt{k_E k_D u(t-u)}\right) e^{-k_E(t-u)-k_D u} \times \left[\sqrt{\frac{D}{\pi u}}\left([\overleftarrow{\partial}_t + k]u - \frac{1}{2}\right)e^{-V^2 u/4D} + \frac{V}{2}\left([\overleftarrow{\partial}_t + k]u - \frac{k_D}{k}\right)\operatorname{erfc}\left(-\sqrt{\frac{V^2 u}{4D}}\right)\right] du. \tag{2.24}$$

2.4.3 Connection to earlier work

2.5 Discussion

2.5.1 The role of stochasticity in landscape evolution

2.5.2 Methods to calculate the sediment flux

2.5.3 Outlook and future research

2.6 Conclusion

Chapter 3

Analysis of the bed elevation

The transport characteristics of coarse grains moving under a turbulent flow ultimately control a wide set processes within rivers, including the export of contaminants (*Macklin et al.*, 2006; *Malmon et al.*, 2005), the success of ecological restoration efforts (*Gaeuman et al.*, 2017), and the response of channel morphology to disturbances (*Hassan and Bradley*, 2017). Although the displacements of individual grains are certainly a mechanical consequence of forces imparted from the flow, bed, and other grains (*González et al.*, 2017; *Vowinckel et al.*, 2014; *Wiberg and Smith*, 1985), accurately characterizing these forces within natural channels is practically impossible, especially considering the intense variability these forces display (*Celik et al.*, 2010; *Dwivedi et al.*, 2011; *Schmeeckle et al.*, 2007). In response, investigators have developed a stochastic concept of bedload transport (*Einstein*, 1937), whereby the erosion and deposition of individual grains are modeled as the random results of undetermined forces (*Ancey et al.*, 2006; *Einstein*, 1950; *Paintal*, 1971).

Essentially two types of bedload transport model have been developed from this concept. The first type provides the probabilistic dynamics of a small population of tracer grains as they transport downstream (*Einstein*, 1937; *Hubbell and Sayre*, 1964; *Lajeunesse et al.*, 2018; *Martin et al.*, 2012; *Nakagawa and Tsujimoto 9 Kyoto*, 1977; *Wu et al.*, 2019a), while the second provides the statistics of the number of moving grains ("the particle activity") within a control volume (*Ancey et al.*, 2006, 2008; *Einstein*, 1950; *Furbish et al.*, 2012b). In the first type, indi-

vidual displacements are considered to result from alternate step-rest sequences, where step lengths and resting times are random variables following statistical distributions (*Einstein*, 1937). Differences between the random-walk motions of one grain and the next imply a spreading apart of tracer grains as they transport downstream: bedload tracers undergo diffusion.

Resting time distributions have been carefully studied in relation to these models because the predicted diffusion characteristics are critically dependent on whether the distribution has a light or heavy tail (*Bradley*, 2017; *Martin et al.*, 2012; *Weeks and Swinney*, 1998). Resting times have puzzled researchers because early experiments show exponential distributions (*Einstein*, 1937; *Hubbell and Sayre*, 1964; *Nakagawa and Tsujimoto 9 Kyoto*, 1977; *Yano*, 1969), while later experiments show heavy-tailed power-law distributions (*Bradley*, 2017; *Liu et al.*, 2019; *Martin et al.*, 2012; *Olinde and Johnson*, 2015; *Voepel et al.*, 2013; **?**). A predominant hypothesis is that power-law distributed resting times originate from buried grains (*Martin et al.*, 2014; *Voepel et al.*, 2013); this hypothesis permits surface grains to retain exponential resting times. Conceptually, when grains rest on the surface, material transported from upstream can deposit on top of them, preventing entrainment until its removal, driving up resting times and imparting a heavy tail to the distribution. To our knowledge, *Martin et al.* (2014) have provided the only direct support for this hypothesis by tracking grains through complete cycles of burial and exhumation using a narrow flume with glass walls. They observed heavy-tailed resting times of buried grains and described their results with a mathematical model similar to an earlier effort by *Voepel et al.* (2013). Both of these models treat bed elevation changes as a random walk and interpret resting times as return periods from above in the bed elevation time-series (*Redner and Dorfman*, 2002). Each describes resting time distributions from different experiments, but they rely on different random walk models, and their treatment of bed elevations as a process independent of sediment transport is questionable at first glance, since bedload transport is the source of bed elevation changes (*Wong et al.*, 2007), and neither model explicitly includes bedload transport. Models of sedimentary bed evolution incorporating sediment transport processes might enhance understanding of sediment resting times.

The second type of stochastic model prescribes rates (probabilities per unit

time) to the erosion and deposition events of individual grains within a control volume to calculate the particle activity (*Einstein*, 1950). These approaches aim at a complete statistical characterization of the bedload flux (*Fathel et al.*, 2015; *Furbish et al.*, 2012b, 2017; *Heyman et al.*, 2016), including probability distributions (*Ancey et al.*, 2006, 2008), spatial and temporal characteristics of its fluctuations (*Ancey et al.*, 2008; *Dhont and Ancey*, 2018; *Heyman*, 2014; *Roseberry et al.*, 2012), and the dependence of these statistical characteristics on the length and time scales over which they are measured or calculated (*Ma et al.*, 2014; *Singh et al.*, 2009, 2012; **?**). A recent surge in research activity has generated rapid progress and spawned many new inquiries in this subject. For example, *Ancey et al.* (2006) demonstrated that a constant erosion rate as originally proposed by *Einstein* (1950) was insufficient to develop realistically large particle activity fluctuations, so they added a positive feedback between the particle activity and erosion rate they called "collective entrainment" (*Ancey et al.*, 2008; *Heyman et al.*, 2013, 2014; *Lee and Jerolmack*, 2018; *Ma et al.*, 2014). While they deemed this feedback necessary to model realistic activity fluctuations, the implications of this collective entrainment term on bed topography and particle activity changes has not been fully explored.

In this work, we present the first stochastic model coupling the erosion and deposition of individual bedload grains to local bed elevation changes. Our model extends the *Ancey et al.* (2008) model to describe the interplay between bedload flux and bed elevation fluctuations in a control volume. This development permits a systematic study of the repercussions of collective entrainment, and it frames bed elevation changes as a direct consequence of the sediment transport process. Our model has two key assumptions: (1) bedload erosion and deposition can be characterized by probabilities per unit time, or rates (*Ancey et al.*, 2008; *Einstein*, 1950); and (2) these rates are contingent on the local bed elevation, encoding the property that erosion of sediment is emphasized from regions of exposure, while deposition is emphasized in regions of shelter (*Wong et al.*, 2007; **?**). We study statistical characteristics of bedload transport, bed elevation, and resting times of sediment undergoing burial using a mixture of numerical simulations and analytical approximations. We introduce the stochastic model in section 4.1, and we solve it in section 4.1.3 with a mixture of numerical and analytical techniques. We discern several new features of particle activity and bed elevation statistics that result from

feedbacks between the erosion and deposition rates and the local bed elevation. We present these features in section 3.3. We conclude with the implications of our results and speculate on topics for future research in sections 4.2 and 4.3.

3.1 Stochastic model of bedload transport and bed elevations

We prescribe a volume of downstream length L containing some number n of moving particles in the flow and some number m of stationary particles composing the bed at time t, as depicted in figure 3.1. We define m relative to the mean number of grains within the control volume, so that it can be either positive or negative. n is always a positive integer including 0. For simplicity, we consider all particles as approximately spherical with the same diameter $2a$, so their mobility and packing characteristics are consistent. Following *Ancey et al.* (2008), we prescribe four events that can occur at any instant to modify the populations n and m, and we characterize these events using probabilities per unit time (rates). These events are (1) migration of a moving particle into the volume from upstream ($n \to n+1$), (2) the entrainment (erosion) of a stationary particle into motion within the volume ($m \to m-1$ and $n \to n+1$), (3) the deposition of a moving particle to rest within the volume ($m \to m+1$ and $n \to n-1$), and (4) the migration of a moving particle out of the volume to downstream ($n \to n-1$). The four events are depicted as arrows in figure 3.1. As the events occur at random intervals, they set up a joint stochastic evolution of the populations n and m characterized by a joint probability distribution $P(n,m,t)$ for the number of particles in motion and rest in the volume at t. The populations n and m provide the bulk bedload flux q_s and the local bed elevation z. The mean bedload transport rate is given by $q_s = u_s\langle n\rangle/L$, where u_s is the characteristic velocity of moving bedload and $\langle n\rangle = \sum_{n,m} nP(n,m)$ is the mean number of grains in motion (*Ancey et al.*, 2008; *Charru et al.*, 2004; *Furbish et al.*, 2012b). The bed elevation is related to m through the packing geometry of the bed. To quantify this, we introduce a packing fraction ϕ of grains in the bed (*Bennett*, 1972), and for simplicity we consider the bed as two-dimensional (*Einstein*, 1950;

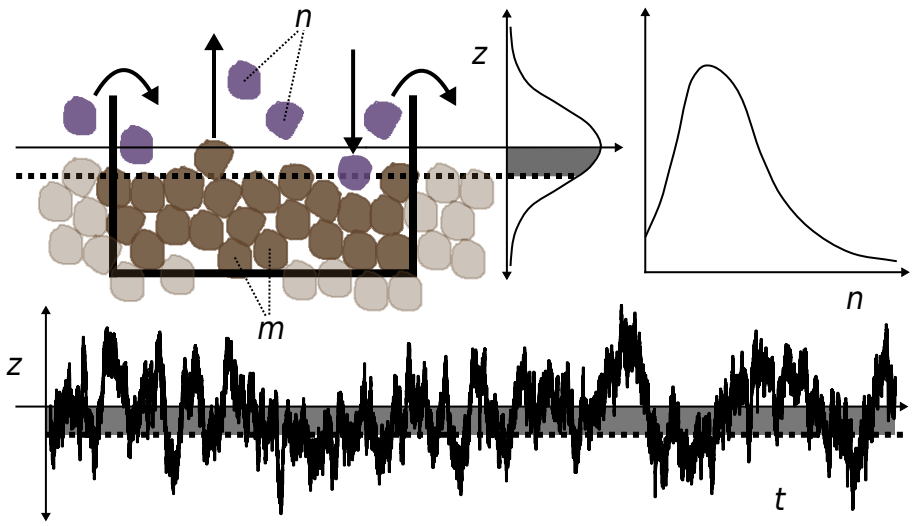

Figure 3.1: Definition sketch of a control volume containing n moving grains and m resting grains. Migration, entrainment, and deposition are represented by arrows, and the instantaneous bed elevation is depicted by dotted lines. The bed is displayed in a degraded state, where $m < 0$. The marginal distributions of n and m are indicated in the upper right panel, while the bottom panel is a realized time-series of bed elevations computed from m using (3.1).

Paintal, 1971). The deviation from the mean bed elevation is then

$$z(m) = \frac{\pi a^2}{\phi L} m = z_1 m. \tag{3.1}$$

The constant $z_1 = \pi a^2/(\phi L)$ is an important scale of the problem. z_1 is the magnitude of bed elevation change in an average sense across the control volume associated with the addition or removal of a single grain.

Bed elevation changes modify the likelihood of entrainment and deposition in a negative feedback (*Wong et al.*, 2007; **?**); that is, aggradation increases the likelihood of entrainment, while degradation increases the likelihood of deposition. *Wong et al.* (2007) concluded that bed elevation changes induce an exponential variation in entrainment and deposition probabilities, while **?** concluded that

the variation is linear. For simplicity, we incorporate the scaling of **?** and note its equivalence to the *Wong et al.* (2007) scaling when bed elevation changes are small. Because experimental distributions of bed elevations are often symmetrical, (*Martin et al.*, 2014; *Pender et al.*, 2001; *Wong et al.*, 2007; **?**), we expect the erosion and deposition feedbacks to have the same strength. That is, as bed elevation changes drive up (down) erosion rates, so they drive down (up) deposition rates to the same degree. Merging these ideas with those of *Ancey et al.* (2008), we write the four possible transitions with local bed elevation-dependent entrainment and deposition rates as

$$R_{MI}(n+1|n) = \nu \qquad \text{migration in,} \tag{3.2}$$

$$R_E(n+1,m-1|n,m) = (\lambda + \mu n)[1+\kappa m], \qquad \text{entrainment,} \tag{3.3}$$

$$R_D(n-1,m+1|n,m) = \sigma n[1-\kappa m], \qquad \text{deposition.} \tag{3.4}$$

$$R_{MO}(n-1|n) = \gamma n \qquad \text{migration out.} \tag{3.5}$$

In equations (3.3) and (3.4), κ is a coupling constant between bed elevations and the entrainment and deposition rates. ν is the rate of migration into the control volume, λ is the conventional entrainment rate, μ is the collective entrainment rate, σ is the deposition rate, and γ is the rate of migration out of the control volume. At $m = 0$, these equations reduce to those of the *Ancey et al.* (2008) model. Away from this elevation, entrainment and deposition are alternatively suppressed and enhanced depending on the sign of m, constituting a feedback between bed elevation changes and erosion and deposition. We refer to κ as a coupling constant since it controls the strength of this feedback. We later demonstrate the relationship

$$\kappa \approx \left(\frac{z_1}{2l}\right)^2 \tag{3.6}$$

where l is a characteristic length scale of bed elevation change that we interpret as the active layer depth (*Correa et al.*, 2017; *Wong et al.*, 2007). All four rates are independent of the past history of the populations and depend only on the current populations (n,m). As a result, the model is Markovian (**??**), meaning time intervals between any two subsequent transitions are exponentially distributed (*Gillespie*, 2007).

We write the master equation for the probability flow using the forward Kolmogorov equation $\partial P(n,m;t)/\partial t = \sum_{n',m'}[R(n,m|n',m')P(n',m';t) - R(n',m'|n,m)P(n,m;t)]$ (*Ancey et al.*, 2008; **?**; **?**) as

$$\begin{aligned}\frac{\partial P}{\partial t}(n,m;t) = \nu P(n-1,m;t) + [\lambda(m+1)+\mu(n-1)][1+\kappa(m+1)]P(n-1,m+1;t) \\ + \sigma(n+1)[1-\kappa(m-1)]P(n+1,m-1;t) + \gamma(n+1)P(n+1,m;t) \\ - \{\nu+\lambda+\mu n(1+\kappa m)+\sigma n(1-\kappa m)+\gamma n\}P(n,m;t). \quad (3.7)\end{aligned}$$

The joint probability distribution $P(n,m;t)$ solving this equation fully characterizes the statistics of n and m – proxies for the bedload flux and local bed elevation. The average entrainment and deposition rates E and D over all bed elevations are $E = \lambda + \mu\langle n\rangle$ and $D = \sigma\langle n\rangle$. We anticipate that solutions of (3.7) will adjust from the initial conditions to a steady-state distribution $P_s(n,m)$ – independent of time – if the constant factors in the transition rates are representative of equilibrium conditions. Equilibrium requires $E = D$, meaning there is no net change in elevation, and $\nu = \gamma\langle n\rangle$, meaning mass is conserved in the control volume (inflow = outflow). This Master equation describes a two-species stochastic birth-death model (**?**) of a type well-known in population ecology (*Pielou*, 2008; *Swift*, 2002) and chemical physics (*Gardiner*, 1983). In our context, the two populations are the moving and stationary grains in the volume.

3.2 Model solutions

Unfortunately, equation (3.7) does not appear to admit an analytical solution unless $\kappa = 0$ (but see *Swift* (2002) for the generating function method which fails in this case). The difficulty originates from the product terms between n and m representing the bed elevation dependence of collective entrainment and deposition rates. In response to this difficulty, we resort to numerical methods and analytical approximations, simulating equation (3.7) with the Gillespie algorithm (*Gillespie*, 1977, 2007; **?**) and solving it approximately with mean field and Fokker-Planck approaches (*Gardiner*, 1983; **?**). The simulation algorithm is described in 3.2.1, and analytical approximations are described in 3.2.2.

3.2.1 Numerical simulations

The Gillespie algorithm leverages the defining property of a Markov process: when transition rates are independent of history, time intervals between transitions are exponentially distributed (**?**). As a result, to step the Markov process through a single transition, one can draw a first random value from the exponential distribution of transition intervals to determine the time of the next transition, then draw a second random value to choose the type of transition that occurs using relative probabilities formed from equations (3.2-3.5). The transition is enacted by shifting t, n and m by the appropriate values to the type of transition (that is, entrainment is $m \to m-1$ and $n \to n+1$, and so on). This procedure can be iterated to form an exact realization of the stochastic process (*Gillespie*, 2007). We provide additional background on the stochastic simulation method in the supplementary material and refer the reader to *Gillespie* (2007) for more detail.

Table 3.1: Migration, entrainment, and deposition rates at $z(m) = 0$ from *Ancey et al.* (2008). Units are s^{-1} (probability/time). In our model, bed elevation changes modulate these rates in accord with (3.2-3.5).

flow	ν	λ	μ	σ	γ
(a)	5.45	6.59	3.74	4.67	0.77
(g)	7.74	8.42	4.34	4.95	0.56
(i)	15.56	22.07	3.56	4.52	0.68
(l)	15.52	14.64	4.32	4.77	0.48

Using this method, we simulated 4 transport conditions with 13 different values of l taken across a range from $l = a$ (a single radius) to $l = 10a$ (10 radii). These values include the range exhibited by the available experimental data on bed elevation timeseries (*Martin et al.*, 2014; *Singh et al.*, 2009; *Wong et al.*, 2007). For the migration, entrainment, and deposition parameters representing bedload transport at each flow condition $(\nu, \lambda, \mu, \sigma, \gamma)$, we used the values measured by *Ancey et al.* (2008) in a series of flume experiments: these are summarized in table 3.1. Flow conditions are labeled (a), (g), (i), and (l), roughly in order of increasing bedload flux (see *Ancey et al.* (2008) for more details). In all simulations, we take the packing fraction $\phi = 0.6$ – a typical value for a pile of spheres (e.g., *Bennett*, 1972), and

we set $L = 22.5$cm and $a = 0.3$cm in accord with the *Ancey et al.* (2008) experiments. Each simulation was run for 250 hours of virtual time, a period selected to ensure neat convergence of particle activity and bed elevation statistics.

3.2.2 Approximate solutions

We approximately decouple the n and m dynamics in equation (3.7) using the inequality $l \gg z_1$ (equivalently $\kappa \ll 1$) which holds for large values of the active layer depth l. These inequalites mean many entrainment or deposition events are required for an appreciable change in the entrainment or deposition rates. We concentrate on steady state conditions $\partial P/\partial t = 0$ and introduce the exact decomposition $P(n,m) = A(n|m)M(m)$ to equation (3.7), with the new distributions normalized as $\sum_m M(m) = 1$ and $\sum_n A(n|m) = 1$. This provides the steady state equation

$$\begin{aligned} 0 = {} & \nu A(n-1|m)M(m) + [\lambda + \mu(n-1)][1+\kappa(m+1)]A(n-1|m+1)M(m+1) \\ & + \sigma(n+1)[1-\kappa(m-1)]A(n+1,m-1)M(m-1) + \gamma(n+1)A(n+1|m)M(m) \\ & - \{\nu + [\lambda+\mu n](1+\kappa m) + \sigma n(1-\kappa m) + \gamma n\}A(n,m)M(m). \quad (3.8) \end{aligned}$$

Summing this equation over n provides a still exact description of the distribution of bed elevations $M(m)$ in terms of the conditional mean particle activity $\langle n|m\rangle = \sum_n nA(n|m)$:

$$\begin{aligned} 0 = {} & [\lambda + \mu\langle n|m+1\rangle][1+\kappa(m+1)]M(m+1) \\ & + \sigma\langle n|m-1\rangle[1-\kappa(m-1)]M(m-1) \\ & - \{[\lambda+\mu\langle n|m\rangle](1+\kappa m) + \sigma\langle n|m\rangle(1-\kappa m)\}M(m). \quad (3.9) \end{aligned}$$

Unforunately, these two equations are no easier to solve than the original master equation, since the coupling between n and m is not reduced in equation (3.8).

The simplest approximation to these equations holds that κ is so small that the dynamics of n are totally independent of m: $A(n|m) = A(n)$. Taking this limit in equation (3.8), summing over m, and using $\langle m\rangle = 0$ reproduces the *Ancey et al.*

(2008) particle activity model. As shown by *Ancey et al.* (2008), this has solution

$$A(n) = \frac{\Gamma(r+n)}{\Gamma(r)n!} p^r (1-p)^n. \tag{3.10}$$

which is a negative binomial distribution for the particle activity with parameters $r = (\nu + \lambda)/\mu$ and $p = 1 - \mu/(\sigma + \gamma)$. This result implies $\langle n|m\rangle = \langle n\rangle$, so with the definitions of E and D and the equilibrium condition $E = D$, equation (3.9) provides

$$0 \approx [1 + \kappa(m+1)]M(m+1) + [1 - \kappa(m-1)]M(m-1) - 2M(m). \tag{3.11}$$

This mean field equation matches the discrete Ornstein-Uhlenbeck model of bed elevation changes developed by *Martin et al.* (2014). We summarize that the independent bed elevation and particle activity models of *Martin et al.* (2014) and *Ancey et al.* (2008) derive from the model we present in a mean field approximation when κ is insignificant.

In the supplementary information we show the Fokker-Planck approximation (*Gardiner*, 1983) formed by expanding $M(m \pm 1)$ to second order in m within equation (3.11) provides the solution $M(m) \propto \exp(-\kappa m^2)$: this is a normal distribution of bed elevations with variance $\sigma_m^2 \propto \frac{1}{2\kappa}$. As we will demonstrate in section 3.3, and as we have already suggested with equation (3.6), this is a poor approximation to the bed elevation variance. Nevertheless, this approximation does capture the Gaussian shape of the bed elevation distribution. The essential issue with this mean field approach is that the conditional mean particle activity $\langle n|m\rangle$ varies significantly with m in actuality, especially when collective entrainment contributes to the mean entrainment rate E. We will discuss these points subsequently when developing more refined approximations and presenting numerical results.

A more careful approximate solution to equation (3.9) can be obtained by prescribing a phenomenological equation for $\langle n|m\rangle$ into equation (3.9) in order to close the equation for m without solving equation (3.8). From numerical simulations we determine that

$$\langle n|m\rangle \approx \langle n\rangle \left(1 - \frac{2\kappa m}{1 - \mu/\sigma}\right) \tag{3.12}$$

captures the general features of the conditional mean particle activity. As we show

in the supplementary information, introducing this closure equation to (3.9), making the Fokker-Planck approximation, and neglecting terms of $O(\kappa^2)$ provides

$$M(m) \approx M_0 e^{-2\kappa m^2}, \tag{3.13}$$

representing a Gaussian distribution with variance $\sigma_m^2 = \frac{1}{4\kappa}$ – smaller than the former mean field theory by a factor of two and in agreement with the result posited in equation (3.6). M_0 is a normalization constant. As we will demonstrate, this closure equation approach shows good coorespondence with numerical solutions of equation (3.7), at least for the flow parameters in table 3.1.

3.3 Results

From the initial conditions, all simulations show a rapid attainment of steady-state stochastic dynamics of n and m which support a time-independent joint distribution $P(n,m)$. We show an elevation time-series in the bottom panel of figure 3.1. In order to describe the implications of coupling bedload transport to bed elevation changes, we present the numerical and analytical results for the probability distributions of bedload transport and bed elevations in section 3.3.1 and the statistical moments of these quantities in section 3.3.2. We isolate the effects of collective entrainment on bed elevation changes in section 3.3.3, and we present the resting times of sediment undergoing burial in section 3.3.4.

3.3.1 Probability distributions of bedload transport and bed elevations

We compute this joint distribution by counting occurrences of the states (n,m) in the simulated time series. From this joint distribution we compute marginal distributions $P(n)$ and $P(m)$ by summing over m and n respectively. A representative subset of these marginal distributions is displayed in figure 4.1 alongside the approximate results of equations (3.10) and (3.13). The mean field equation (3.10) for the particle activity n closely represents the numerical results, and while there are small differences between numerical and analytical results for the relative number m of resting particles, the numerical solutions approximately match equation

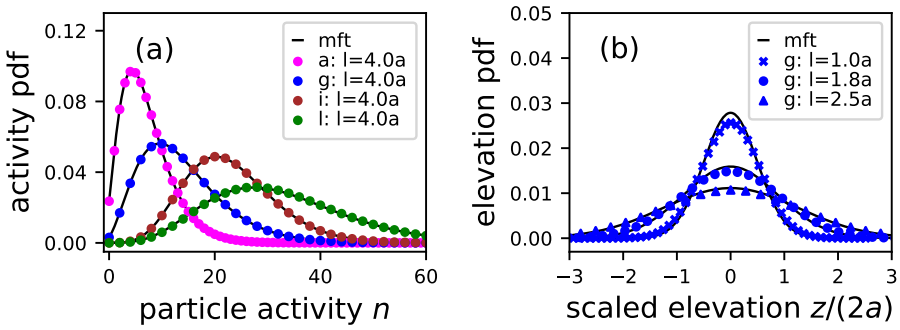

Figure 3.2: Panel (a) presents the probability distribution of particle activity n and panel (b) presents the probability distribution of the relative number of particles m for a representative subset of simulations. These distributions represent different flows from table 3.1, distinguished by color, and different values of the active layer depth l (equivalently the coupling constant κ), distinguished by the marker style. The mean field theories (mft) of equations (3.10) and (3.13) are displayed as solid black lines.

(3.13), having Gaussian profiles consistent with our assumption of a symmetric scaling of erosion and deposition rates with bed elevation changes.

3.3.2 Statistical moments

We calculate the moments of n and m by summing over $P(n,m)$. The jth order unconditional moment of the particle activity n derives from

$$\langle n^j \rangle = \sum_n n^j P(n), \tag{3.14}$$

while the jth order moment of n held conditional on m is

$$\langle n^j | m \rangle = \sum_n n^j P(n,m). \tag{3.15}$$

We observe no dependence of the moments of m on the value of n. The mean elevation is always $\langle m \rangle = 0$ due to our initial assumption of symmetry in the entrainment and deposition rate scaling with m. Figure 4.2 demonstrates that the variance of bed elevations is approximately $\sigma_z^2 = z_1^2 \sigma_m^2 = \frac{1}{4\kappa} = l^2$, agreeing with the approximation in equation (3.13); this result supports our earlier assertion that l is a characteristic length scale of bed elevation fluctuations. The close correspondence between the mean field approximation and the numerical simulations in figure (4.1a) suggests the unconditional moments of n correspond closely with the *Ancey et al.* (2008) result. We find them to be identical within numerical uncertainty.

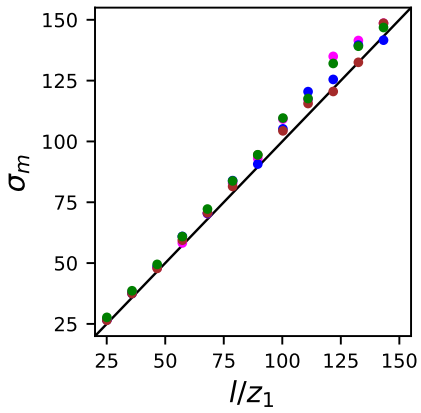

Figure 3.3: Data from all simulations demonstrating that the active layer depth l characterizes bed elevation changes as posited in equation (3.6): $\sigma_m^2 \approx (l/z_1)^2$.

The coupling between bed elevation changes and the erosion and deposition rates develop a strong dependence of the particle activity on m. Figure (3.4) displays the mean shift $[\langle n|m \rangle - \langle n \rangle]/\langle n \rangle$ and the variance shift $[\mathrm{var}(n|m) - \mathrm{var}(n)]/\mathrm{var}(n)$ of the particle activity due to departures of the bed elevation from its mean position. Figure (3.4a) demonstrates that the *Ancey et al.* (2008) flow conditions support departures of the mean particle activity by as much as 60% from the overall mean value when the bed is in a degraded state $z \approx -3l$, and the activity can be decreased by 20% when the bed is in an aggraded state. The closure model (3.12) used to derive the approximate bed elevation distribution (3.13) is plotted behind the conditional mean profiles in figure (3.4a), where it appears to be crude approximation, as it does not capture the asymmetry in this quantity. Nevertheless, figure 4.2 demonstrates the variance $1/(4\kappa)$ derived from this closure equation is representative of the numerical relationship. For the parameters of the *Ancey et al.* (2008) experiments, figure (3.4b) displays a variance shift with bed eleva-

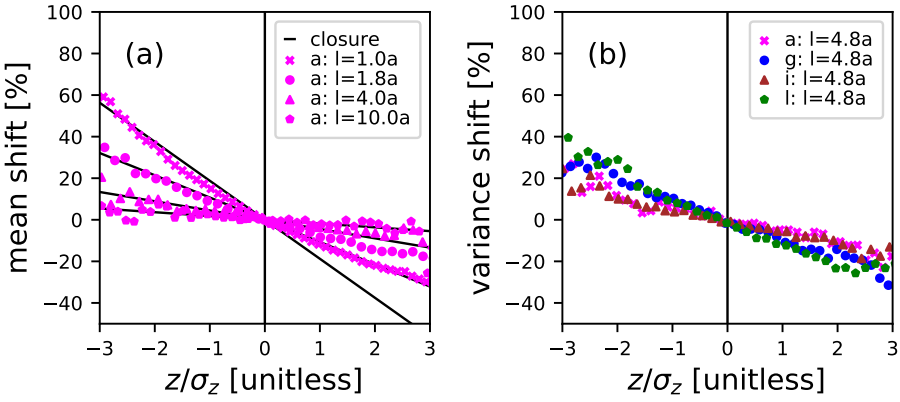

Figure 3.4: The shifts between particle activity moments conditioned on instantaneous elevations and their over-all mean values. Panel (a) indicates the mean particle activity shift versus the bed elevation measured in units of $\sigma_z = l$. This shift displays asymmetric dependence on m at the flow conditions of the *Ancey et al.* (2008) experiements, and departures of the bedload transport mean can be as much as 60% when the bed is in a severely degraded state with $z \approx -3l$. The closure equation (3.12) is plotted in panel (a) Panel (b) demonstrates a more symmetrical variance shift with some dependence on flow conditions displaying shifts of up to 20% with bed elevations. These results indicate that bedload statistics measurements on short timesclaes could be severely biased by departures from the mean bed elevation.

tion changes that is less severe than the mean shift but is nevertheless appreciable, with bed elevations changing the magnitude of bedload activity fluctuations by as much as 20%. We summarize that bed elevation changes regulate the particle activity moments, with a moment suppression effect when the bed is aggraded, and a moment enhancement effect when the bed is degraded.

3.3.3 Collective entrainment and bedload activity fluctuations

Noting that bed elevations regulate the particle activity moments, we now study the influence of collective entrainment on this effect by modifying the relative proportion of the individual to collective contributions in the mean entrainment rate

$E = \lambda + \sigma\langle n \rangle$. Using the equilibrium condition $E = D$, we determine the fraction of entrainment due to the collective process is $f = \mu\langle n \rangle / E = \mu/\sigma$. Using this fraction, we can hold E constant and modify the prevalence of the collective entrainment process by setting $\lambda = E(1-f)$ and $\mu = \sigma f$. As we interpolate f between zero and one, the particle activity component of the master equation 3.7 interpolates from a purely Poissonian model (*Ancey et al.*, 2006) to a negative binomial model (*Ancey et al.*, 2008), isolating the imprint of collective entrainment on particle activity statistics over a dynamic sedimentary bed. Figure 3.5 depicts

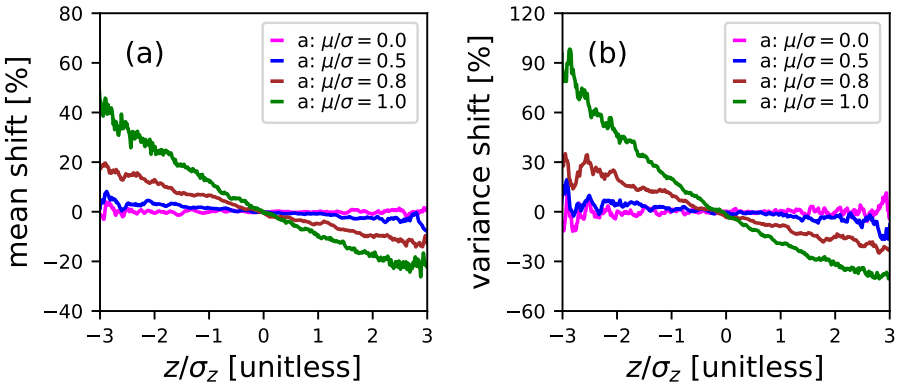

Figure 3.5: The shift of the mean particle activity in panel (a) and its fluctuations in panel (b) with departures of the bed elevation from its mean. All simulations are at flow condition (g) from table 3.1 except λ and μ are modified to shift the fraction $f = \mu/\sigma$ of the over-all entrainment rate E due to collective entrainment. Clearly, collective entrainment drives strong departures of the bedload statistics away from the mean field model (3.10) at large departures from the mean bed elevation. Panel (b) shows particle activity fluctuations suppressed by 90% when $z \approx -3l$ and collective entrainment is the dominant process. When collective entrainment is absent, meaning $\mu/\sigma = 0$, this moment regulation effect vanishes: it is a consequence of collective entrainment.

the modification of the particle activity mean and variance as the importance of collective entrainment is tuned (through λ and μ) with all other parameters fixed. When $f = 0$, the bed elevation ceases to influence the particle activity mean or

variance, while larger fractions increasingly enable the moment regulation effect we introduced in section 3.3.2.

3.3.4 Resting times of sediment undergoing burial

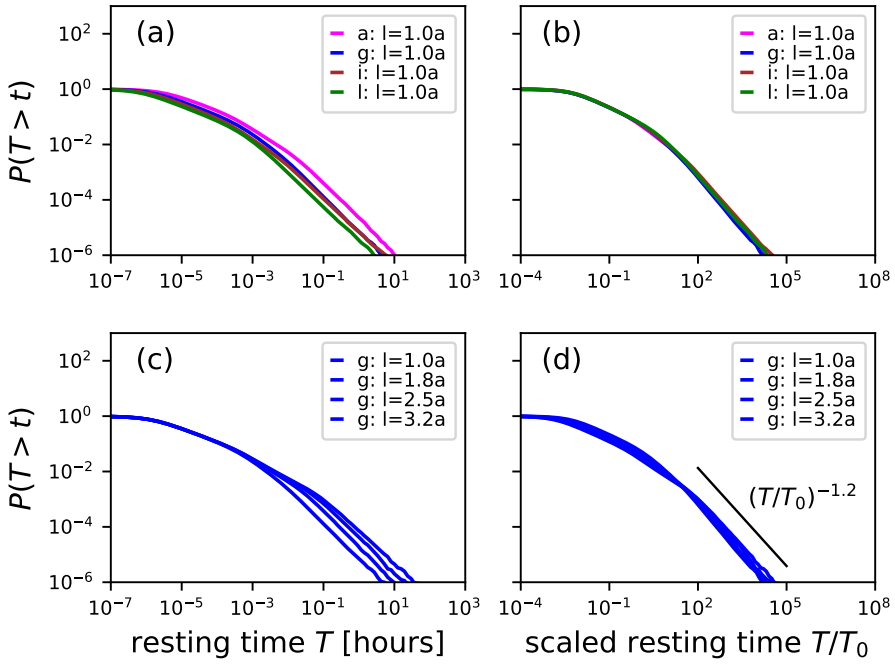

Figure 3.6: Resting time statistics scale differently with transport conditions and the bed elevation variance. Panel (a) shows differing flow conditions at a fixed l value, while panel (c) shows fixed flow conditions at differing l. When scaled by T_0 (3.17), both types of difference collapse in the tails of the distributions, as shown in panels (b) and (d). In panels (b) and (d), the black dotted lines indicate a power law decay of the collapsed tails having parameter $\alpha \approx 1.18$.

Resting times for sediment undergoing burial are obtained from analyzing the return times from above in the time-series of m (e.g., *Redner and Dorfman*, 2002). Following *Voepel et al.* (2013) and *Martin et al.* (2014), we concentrate on a particular bed elevation m', and find all time intervals separating deposition events at

$m = m'$ from erosion events at $m = m' + 1$. These are the return times from above of the sedimentary bed conditional to the elevation m'. Binning these conditional return times (using logarithmically-spaced bins to reduce computational load) and counting the occurrences in each bin, we obtain an exceedance distribution of return times t_r held conditional to the elevation m': $P(T > t_r|m')$. Using the marginal probability distribution of bed elevations $P(m)$ (figure 4.1(b)), we derive the unconditional exceedance distribution of resting times as a sum over all elevations (*Martin et al.*, 2014; *Voepel et al.*, 2013; *Yang and Sayre*, 1971; **?**):

$$P(T > t_r) = \sum_{m'} P(m')P(T > t_r|m'). \tag{3.16}$$

A representative subset of these results are displayed in figure 3.6. Comparing panels 3.6(a) and 3.6(c) shows two separate variations with input parameters: first, the distributions vary with the flow conditions, and second, they vary with the standard deviation of bed elevations (l). However, as shown in panels 3.6(b) and 3.6(d), a characteristic timescale T_0 is found to collapse away both variations. We obtained this T_0 heuristically by considering the characteristic speed of bed elevation change. This is the mean number of grains leaving the bed per unit time is E, and the removal of a single grain changes the bed elevation by z_1 (3.1). Therefore, bed elevations change with a characteristic speed $v = z_1 E$. Since the range of elevation deviations is l (figure 4.2), the time required for the bed to shift through this characteristic distance is l/v, or equivalently

$$T_0 = \frac{l}{z_1 E}. \tag{3.17}$$

When scaling the resting time by this T_0, we obtain the collapse shown in figure 3.6. Using the log-likelihood estimation technique described by *Newman* (2005), we estimate the scaled resting time non-exceedance distributions decay as a heavy tailed power law with parameter $\alpha = 1.18 \pm 0.32$ for all return times satisfying $T/T_0 > 10^3$. These distributions are sufficiently heavy tailed to violate the central limit theorem and drive anomalous super-diffusion of bedload, a result which supports the earlier conclusions of *Voepel et al.* (2013) and *Martin et al.* (2014).

3.4 Discussion

3.4.1 Context

Einstein developed the first stochastic models of bedload tracer diffusion (*Einstein*, 1937) and the bedload flux (*Einstein*, 1950), and his ideas can be viewed as the nexus of an entire paradigm of research that extends into the present day (e.g., *Ancey et al.*, 2008; *Hassan et al.*, 1991; *Hubbell and Sayre*, 1964; *Nakagawa and Tsujimoto 9 Kyoto*, 1977; *Wu et al.*, 2019a). These models aim to predict bedload transport characteristics from stochastic concepts of individual particle motions. With some exceptions (*Shi and Wang*, 2014; *Wu et al.*, 2019a,b; *Yang and Sayre*, 1971; **?**), existing descriptions are spatially one-dimensional, concentrating on the motion of grains in the downstream direction without including the vertical dimension wherein local bed elevation changes imply sediment burial (*Martin et al.*, 2014; *Voepel et al.*, 2013) and change the mobility of surface grains (*Yang and Sayre*, 1971; **?**).

3.4.2 Contributions

In this paper, we have built on earlier works (*Ancey et al.*, 2008; *Martin et al.*, 2014) to include the vertical dimension of bed elevation dynamics, study the interplay between bedload transport and bed elevation fluctuations, and investigate resting time distributions of sediment undergoing burial. To our knowledge, this model is the first description of bedload transport and bed elevations as a coupled stochastic population model based on individual grains. Numerical solutions and analytical approximations provided negative binomial distributions of bedload activity and normal distributions of bed elevations. Although experiments under more natural conditions with segregation processes, migrating bedforms, or sediment supply perturbations have shown particle activity distributions with heavier tails (*Dhont and Ancey*, 2018; **?**) and non-Gaussian bed elevations (*Aberle and Nikora*, 2006; *Singh et al.*, 2012), our results reproduce the key features of the most controlled bed elevation (*Martin et al.*, 2014; *Wong et al.*, 2007) and bedload transport (*Ancey et al.*, 2008; *Heyman et al.*, 2016) experiments in the literature.

Our inclusion of coupling between the bed elevation and entrainment and de-

position rates revealed a novel dependence of particle activity on bed elevation changes, highlighting a new consequence of the collective entrainment process (*Ancey et al.*, 2008; *Lee and Jerolmack*, 2018). This coupling develops a significant variation of the particle activity moments with deviations of the bed from its mean elevation. We isolated the role of collective entrainment in this bedload activity regulation, and pointed out that particle activity variations with bed elevations dissapear in the absence of collective entrainment. Finally, we obtained resting times for sediment undergoing burial within the sedimentary bed by analyzing return times from above in the bed elevation time-series. We found heavy-tailed power law resting times with tail parameters sufficient to drive anomalous diffusion of bedload at long timescales. The distribution tails were found to collapse across flow conditions using a timescale formed from the mean erosion rate and the active layer depth.

As our model builds on earlier works describing particle activity and bed elevation changes independently, it also reduces to these works in simplified limits when the coupling between the particle activity and bed elevation vanishes. With the mean field approach in section 3.2.2, we derived the *Martin et al.* (2014) Ornstein-Uhlenbeck model for bed elevations and the *Ancey et al.* (2008) birth-death model for the particle activity as simplified limits of our coupled model. While the mean field description of bed elevations over-predicts the bed elevation variance by approximately a factor of two, it does capture the Gaussian shape of the bed elevation distribution, and its conclusions on the tail characteristics of resting time distributions for sediment undergoing burial are identical to ours within the numerical uncertainty: *Martin et al.* (2014) described a power-law distribution with tail parameter $\alpha \approx 1$ which falls neatly within our estimation $\alpha = 1.18 \pm 0.32$. In addition to our original contributions, we have corroborated the models of *Ancey et al.* (2008) and *Martin et al.* (2014) from an alternate perspective, showing their results to be mostly robust when accounting for bed elevation changes.

3.4.3 Next steps

The model we have presented computes statistical characteristics of the bedload particle activity and bed elevation within a control volume by assuming all particles

on the bed surface have similar mobility characteristics while sediment transport and bed topography are in equilibrium. In actuality, particles span a range of sizes, and spatial organization occurs both in the forces imparted to particles by the flow (*Amir et al.*, 2014; *Shih et al.*, 2017) and in the mobility characteristics of particles on the bed surface (*Charru et al.*, 2004; *Hassan et al.*, 2007; *Nelson et al.*, 2014). Together, these factors may generate spatial correlations in particle activities that models concentrating on a single control volume will be unable to capture. Models chaining multiple control volumes together have shown spatial correlations in the particle activity as a result of collective entrainment (*Ancey et al.*, 2015; *Heyman et al.*, 2014), and similar approaches have also been applied to study correlations in turbulent flows (*Gardiner*, 1983). In light of this work, we consider the model we have presented as a preliminary step toward a multiple-cell model of particle activities and bed elevation changes with potential to express spatial correlations between longitudinal profile and particle activity statistics.

Like *Martin et al.* (2014), we obtained heavy-tailed power-law resting times for sediment undergoing burial by treating bed elevation changes as an unbounded random walk with a mean reverting tendency. This result suggests sediment burial can explain the heavy-tailed rests seen in field data (*Bradley*, 2017; *Olinde and Johnson*, 2015; **?**). Our resting time distributions show a divergent variance and possibily a divergent mean, since this occurs for $\alpha < 1$ (**?**) which is within range of our results. Divergent mean resting time distributions present a paradox, since they imply all particles should eventually be immobile, violating the equilibrium transport assumption. *Voepel et al.* (2013) demonstrated that a bounded random walk for bed elevations provides a power-law distribution that eventually transitions to a faster thin-tailed decay, allowing for power-law scaling like our result and *Martin et al.* (2014) without this divergent mean paradox. One resolution to this issue could come from a spatially distributed model with multiple cells. Neighboring locations might bound excessive local elevation changes through granular relaxations from gradients above the angle of repose. In this interpretation, divergent mean power law resting time distributions may be relics of single cell models for bed elevation changes. We should always expect a maximum depth to which the bed can degrade relative to neighboring locations; this could temper the power law tail without required the reflecting boundaries used by *Voepel et al.* (2013).

Finally, we studied probability distribution functions and first and second moments of the particle activity and bed elevation, making novel conclusions about coordination between the statistical characteristics of these quantites which deserve experimental testing. In the last decade, particle tracking experiments have emerged (*Fathel et al.*, 2015; *Heyman et al.*, 2016; *Lajeunesse et al.*, 2010; *Liu et al.*, 2019; *Martin et al.*, 2014; *Roseberry et al.*, 2012), that allow joint resolution of bed elevations and bedload transport. A suitably designed experiment could test our prediction that bed elevations regulate particle activity statistics, as essentially represented in figures 3.4 and 3.5. However, we have left many other statistical characteristics of bedload transport for future studies. For example, the dependence of bedload transport (*Singh et al.*, 2009; **?**) and bed elevation statistics (*Aberle and Nikora*, 2006; *Singh et al.*, 2009, 2012) on the spatial and temporal scales over which they are observed is an emerging research topic. Statistical quantities can either be monoscaling or multiscaling across the observation scale (**?**), and we currently lack physical understanding and general conclusions about the scale dependence of particle activity and bed elevation signals. The model we have presented shows statistical monoscaling for both quantites (e.g. **?**), whereas other experiments indicate statistical multiscaling (*Aberle and Nikora*, 2006; *Singh et al.*, 2009, 2012). We consider this topic to go beyond the scope of the present work, and we have focused on statistical characteristics at the highest temporal resolutions, with no averaging over the observation scale.

3.5 Conclusion

We developed a stochastic model for particle activity and local bed elevations including feedbacks between elevation changes and the erosion and deposition rates. This model includes collective entrainment, whereby moving particles tend to destabilize stationary ones. We analyzed this model using a mixture of numerical and analytical methods and provided two key results:

1. Resting times for sediment undergoing burial lie on a heavy-tailed power law distributions with tail parameter $\alpha \approx 1.2$;

2. Collective entrainment generates a statistical regulation effect, whereby bed

elevation changes modify the mean and variance of the particle activity by as much as 90%: this effect vanishes when collective entrainment is absent.

These results imply measurements of bedload transport statistics could be severely biased at observation timescales smaller than adjustments of the bed elevation time-series when collective entrainment occurs. Next steps are to generalize our model to a multi-cell framework and to study spatial correlations in bed elevation and particle activity statistics.

Chapter 4

Inclusion of sediment burial

Many environmental problems including channel morphology (*Hassan and Bradley*, 2017), contaminant transport (*Macklin et al.*, 2006), and aquatic habitat restoration (*Gaeuman et al.*, 2017) rely on our ability to predict the diffusion characteristics of coarse sediment tracers in river channels. Diffusion is quantified by the time dependence of the positional variance σ_x^2 of a group of tracers. With the scaling $\sigma_x^2 \propto t$, the diffusion is said to be normal, since this is found in the classic problems (*Philip*, 1968). However, with the scaling $\sigma_x^2 \propto t^\gamma$ with $\gamma \neq 1$, the diffusion is said to be anomalous (*Sokolov*, 2012), with $\gamma > 1$ defining super-diffusion and $\gamma < 1$ defining sub-diffusion (*Metzler and Klafter*, 2000). *Einstein* (1937) developed one of the earliest models of bedload diffusion to describe a series of flume experiments (**?**). Interpreting individual bedload trajectories as a sequence of random steps and rests, Einstein originally concluded that a group of bedload tracers undergoes normal diffusion.

More recently, Nikora et al. realized coarse sediment tracers can show either normal or anomalous diffusion depending on the length of time they have been tracked (*Nikora et al.*, 2001, 2002). From numerical simulations and experimental data, Nikora et al. discerned "at least three" scaling ranges $\sigma_x^2 \propto t^\gamma$ as the observation time increased. They associated the first range with "local" timescales less than the interval between subsequent collisions of moving grains with the bed, the second with "intermediate" timescales less than the interval between successive resting periods of grains, and the third with "global" timescales composed of many

intermediate timescales. Nikora et al. proposed super-diffusion in the local range, anomalous or normal diffusion in the intermediate range, and sub-diffusion in the global range. They attributed these ranges to "differences in the physical processes which govern the local, intermediate, and global trajectories" of grains (*Nikora et al.*, 2001), and they called for a physically based model to explain the diffusion characteristics (*Nikora et al.*, 2002).

Experiments support the Nikora et al. conclusion of multiple scaling ranges (*Fathel et al.*, 2016; *Martin et al.*, 2012), but they do not provide consensus on the expected number of ranges or their scaling properties. This lack of consensus probably stems from resolution issues. For example, experiments have tracked only moving grains, resolving the local range (*Fathel et al.*, 2016; *Furbish et al.*, 2012a, 2017); grains resting on the bed surface between movements, resolving the intermediate range (*Einstein*, 1937; *Nakagawa and Tsujimoto 9 Kyoto*, 1977; *Yano*, 1969); grains either moving or resting on the bed surface, likely resolving local and intermediate ranges (*Martin et al.*, 2012); or grains resting on the surface after floods, likely resolving the global range (*Bradley*, 2017; *Phillips et al.*, 2013). At long timescales, a significant fraction of tracers bury under the bed surface (*Ferguson et al.*, 2002; *Haschenburger*, 2013; *Hassan et al.*, 1991, 2013; *Papangelakis and Hassan*, 2016), meaning burial dominates long term diffusion characteristics (*Bradley*, 2017; *Martin et al.*, 2014; *Voepel et al.*, 2013), possibly at global or even longer "geomorphic" timescales (*Hassan and Bradley*, 2017) than Nikora et al. originally considered. As a result, three diffusion ranges can be identified by patching together multiple datasets (*Nikora et al.*, 2002; *Zhang et al.*, 2012), but they are not resolved by any one dataset.

Newtonian bedload trajectory models also show multiple diffusion ranges, although they also do not provide consensus on the expected number of ranges or their scaling properties. The majority of these models predict two ranges of diffusion (local and intermediate) without predicting a global range. Among these, *Nikora et al.* (2001) used synthetic turbulence (*Kraichnan*, 1970) with a discrete element method for the granular phase (**?**); *Bialik et al.* (2012) used synthetic turbulence with a random collision model (*Sekine and Kikkawa*, 1992); and *Fowler* (2016) used a Langevin equation with probabilistic rests. To our knowledge, only *Bialik et al.* (2015) have claimed to capture all three ranges from a Newtonian ap-

proach. They incorporated a second resting mechanism into their earlier model (*Bialik et al.*, 2012), implicitly suggesting that three diffusion ranges could result from two distinct timescales of sediment rest. However, Newtonian approaches have not evaluated the effect of sediment burial on tracer diffusion, probably due to the long simulation timescales required.

Random walk bedload diffusion models constructed in the spirit of *Einstein* (1937) provide an alternative to the Newtonian approach and can include a second timescale of rest by incorporating sediment burial. Einstein originally modeled bedload trajectories as instantaneous steps interrupted by durations of rest lying on statistical distributions (*Hassan et al.*, 1991), but this generates only one range of normal diffusion (*Einstein*, 1937; *Hubbell and Sayre*, 1964; *Nakagawa and Tsujimoto 9 Kyoto*, 1977). Recently, researchers have generalized Einstein's model in a few different ways to describe multiple diffusion ranges. *Lisle et al.* (1998) and **?** promoted Einstein's instantaneous steps to motion intervals with random durations and a constant velocity, providing two diffusion ranges – local and intermediate. *Wu et al.* (2019a) retained Einstein's instantaneous steps but included the possibility that grains can become permanently buried as they rest on the bed, also providing two diffusion ranges – intermediate and global. These earlier works suggest the minimal required components to model three bedload diffusion ranges: (1) exchange between motion and rest intervals and (2) the sediment burial process.

In this study, we incorporate these two components into Einstein's original approach to describe three diffusion ranges with a physically based model, as called for by *Nikora et al.* (2002). Einstein was a giant in river geophysics and fostered an entire paradigm of research leveraging and generalizing his stochastic methods (*Gordon et al.*, 1972; *Hubbell and Sayre*, 1964; *Nakagawa and Tsujimoto 9 Kyoto*, 1977; *Paintal*, 1971; *Yang and Sayre*, 1971; *Yano*, 1969). Einstein's model can be viewed as a pioneering application of the continuous time random walk (CTRW) developed by *Montroll* (1964) in condensed matter physics to describe the diffusion of charge carriers in solids. To incorporate motion intervals and sediment burial, we utilize the multi-state CTRW developed by *Weiss* (1976, 1994) that extends the CTRW of *Montroll* (1964). Below, we develop and solve the model in section 4.1. Then, we discuss the predictions of our model, present its implications for local, intermediate, and global ranges of bedload diffusion, and suggest next steps for

bedload diffusion research in sections 4.2 and 4.3.

4.1 Bedload trajectories as a multi-state random walk

4.1.1 Model assumptions

We construct a three-state random walk where the states are motion, surface rest, and burial, and we label these states as $i = 2$ (motion), $i = 1$ (rest), and $i = 0$ (burial). Our target is the probability distribution $p(x,t)$ to find a grain at position x and time t if we know it started with the initial distribution $p(x,0) = \delta(x)$. We characterize times spent moving or resting on the surface by exponential distributions $\psi_2(t) = k_2 e^{-k_2 t}$ and $\psi_1(t) = k_1 e^{-k_1 t}$, since numerous experiments show thin-tailed distributions for these quantities (*Ancey et al.*, 2006; *Einstein*, 1937; *Fathel et al.*, 2015; *Martin et al.*, 2012; *Roseberry et al.*, 2012). We expect our conclusions will not be contingent on the specific distributions chosen, since all thin-tailed distributions provide similar diffusion characteristics in random walks (*Weeks and Swinney*, 1998; *Weiss*, 1994). We consider grains in motion to have characteristic velocity v (*Lisle et al.*, 1998; **?**), and we model burial as long lasting enough to be effectively permanent (*Wu et al.*, 2019a), with grains resting on the surface having a probability per unit time κ to become buried, meaning $\Phi(t) = e^{-\kappa t}$ represents the probability that a grain is not buried after resting for a time t, while $1 - \Phi(t)$ represents the probability that it is buried. We specify the initial conditions with probabilities θ_1 and θ_2 to be in rest and motion at $t = 0$, and we require $\theta_1 + \theta_2 = 1$ for normalization.

4.1.2 Governing equations

Using these assumptions, we derive the governing equations for the set of probabilities $\omega_{ij}(x,t)$ that a transition occurs from state i to state j at position x and time t using the statistical physics approach to multi-state random walks (*Schmidt et al.*, 2007; *Weeks and Swinney*, 1998; *Weiss*, 1994). Denoting by $g_{ij}(x,t)$ the probability for a particle to displace by x in a time t within the state i before it transitions to the state j, the transition probabilities $\omega_{ij}(x,t)$ sum over all possible paths to the state

i from previous locations and times:

$$\omega_{ij}(x,t) = \theta_i g_{ij}(x,t) + \sum_{k=0}^{2} \int_0^x dx' \int_0^t dt' \omega_{ki}(x',t') g_{ij}(x-x',t-t'). \tag{4.1}$$

Defining another set of probabilities $G_i(x,t)$ that a particle displaces by a distance x in a time t within the state i and possibly remains within the state, we perform a similar sums over paths for the probabilities to be in the state i at x, t:

$$p_i(x,t) = \theta_i G_i(x,t) + \sum_{k=0}^{2} \int_0^x dx' \int_0^t dt' \omega_{ki}(x',t') G_i(x-x',t-t'). \tag{4.2}$$

Finally, the overall probability to be at position x at time t is

$$p(x,t) = \sum_{k=0}^{2} p_k(x,t) \tag{4.3}$$

This joint density is completely determined from the solutions of equations (4.1-4.2). We only need to specify the distributions g_{ij} and G_i.

4.1.3 Joint probability distribution

We construct these distributions from the assumptions described in section 4.1.1. Since particles resting on the bed surface bury in a time t with probability $\Phi(t)$, and resting times are distributed as $\psi_1(t)$, we obtain $g_{12}(x,t) = \delta(x) k_1 e^{-k_1 t} e^{-\kappa t}$ and $g_{10}(x,t) = \delta(x) k_1 e^{-k_1 t}(1 - e^{-\kappa t})$. Since motions have velocity v for times distributed as $\psi_2(t)$, we have $g_{21}(x,t) = \delta(x - vt) k_2 e^{-k_2 t}$. Since burial is quasi-permanent, all other $g_{ij} = 0$. The G_i are constructed in the same way except using the cumulative probabilities $\int_t^\infty dt' \psi_i(t) = e^{-k_i t}$, since these characterize motions and rests that are ongoing (*Weiss*, 1994). We obtain $G_1(x,t) = \delta(x) e^{-k_1 t}$ and $G_2(x,t) = \delta(x - vt) e^{-k_2 t}$.

To solve equations (4.1-4.2) with these g_{ij} and G_i, we take Laplace transforms in space and time $(x,t \to \eta,s)$ using a method similar to *Weeks and Swinney* (1998) to unravel the convolution structure of these equations, eventually obtaining

$$\tilde{p}(\eta,s) = \frac{1}{s} \frac{(s+\kappa+k')s + \theta_1(s+\kappa)\eta v + \kappa k_2}{(s+\kappa+k_1)\eta v + (s+\kappa+k')s + \kappa k_2}, \tag{4.4}$$

where $k' = k_1 + k_2$. Inverting this result using known Laplace transforms (*Arfken*, 1985; *Prudnikov et al.*, 1988) obtains

$$\begin{aligned} p(x,t) = \theta_1 \Big[1 - \frac{k_1}{\kappa + k_1}\Big(1 - e^{-(\kappa+k_1)t}\Big)\Big]\delta(x) \\ + \frac{1}{v} e^{-\Omega\tau - \xi}\Big(\theta_1\Big[k_1 \mathscr{I}_0\big(2\sqrt{\xi\tau}\big) + k_2\sqrt{\frac{\tau}{\xi}}\mathscr{I}_1\big(2\sqrt{\xi\tau}\big)\Big] \\ + \theta_2\Big[k_1\delta(\tau) + k_2\mathscr{I}_0\big(2\sqrt{\xi\tau}\big) + k_1\sqrt{\frac{\xi}{\tau}}\mathscr{I}_1\big(2\sqrt{\xi\tau}\big)\Big]\Big) \\ + \frac{1}{v}\frac{\kappa k_2}{\kappa + k_1} e^{-\kappa\xi/(\kappa+k_1)}\Big[(\theta_1/\Omega)\mathscr{Q}_2(\xi/\Omega, \Omega\tau) + \theta_2 \mathscr{Q}_1(\xi/\Omega, \Omega\tau)\Big] \end{aligned} \tag{4.5}$$

for the joint distribution that a tracer is found at position x at time t. This result generalizes the earlier results of *Lisle et al.* (1998) and *Einstein* (1937) to include sediment burial. In this equation, we used the shorthand notations $\xi = k_2 x/v$, $\tau = k_1(t - x/v)$, and $\Omega = (\kappa + k_1)/k_1$ (*Lisle et al.*, 1998). The $\mathscr{I}_\nu$ are modified Bessel functions of the first kind and the $\mathscr{Q}_\mu$ are generalized Marcum Q-functions defined by $\mathscr{Q}_\mu(x,y) = \int_0^y e^{-z-x}(z/x)^{(\mu-1)/2}\mathscr{I}_{\mu-1}(2\sqrt{xz})dz$ and originally devised for radar detection theory (*Marcum*, 1960; *Temme and Zwillinger*, 1997). The Marcum Q-functions derive from the burial process. Since we assumed resting grains could bury with an exponential probability while the resting probability follows a modified Bessel distribution (*Einstein*, 1937; *Lisle et al.*, 1998), burial develops the Q-function convolution structure.

Figure 4.1 depicts the distribution (4.5) alongside simulations generated by a direct method based on evaluating the cumulative transition probabilities between states on a small timestep (*Barik et al.*, 2006). When grains do not become buried, as in panel (a) of figure 4.1, the distribution becomes Gaussian-like at relatively large observation times, exemplifying normal diffusion and satisfying the central limit theorem. When grains become buried, as in panel (b) of figure 4.1, the Q-function terms prevent the distribution from approaching a Gaussian at large timescales, exemplifying anomalous diffusion (*Weeks and Swinney*, 1998) and violating the central limit theorem (*Metzler and Klafter*, 2000; *Schumer et al.*, 2009).

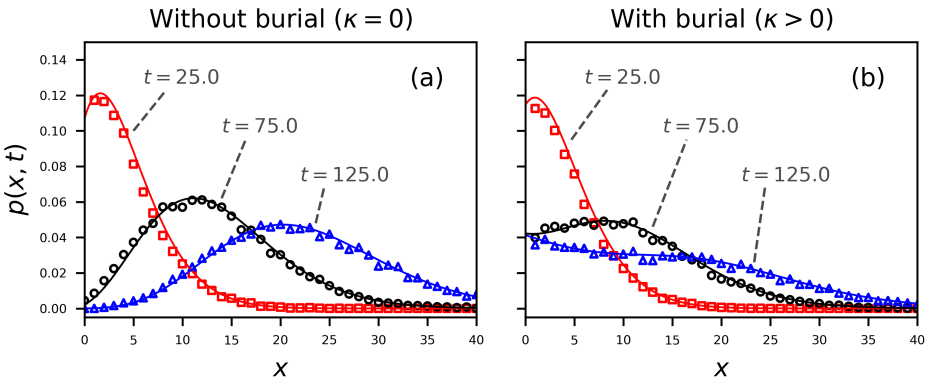

Figure 4.1: Joint distributions for a grain to be at position x at time t are displayed for the choice $k_1 = 0.1$, $k_2 = 1.0$, $v = 2.0$. Grains are considered initially at rest ($\theta_1 = 1$, $\theta_2 = 0$). The solid lines are the analytical distribution in equation (4.5), while the points are numerically simulated, showing the correctness of our derivations. Colors pertain to different times. Units are unspecified, since we aim to demonstrate the general characteristics of $p(x,t)$. Panel (a) shows the case $\kappa = 0$ – no burial. In this case, the joint distribution tends toward Gaussian at large times (*Einstein*, 1937; *Lisle et al.*, 1998). Panel (b) shows the case when grains have rate $\kappa = 0.01$ to become buried while resting. Because of burial, the joint distribution tends toward a more uniform distribution than Gaussian.

4.1.4 Positional variance

To obtain an analytical formula for tracers diffusing downstream while they gradually become buried, we derive the first two moments of position by taking derivatives with respect to η of the Laplace space distribution (4.4) using an approach similar to *Shlesinger* (1974) and *Weeks and Swinney* (1998), and we use these to calculate the positional variance $\sigma_x^2 = \langle x^2 \rangle - \langle x \rangle^2$. The first two moments are

$$\langle x(t) \rangle = A_1 e^{(b-a)t} + B_1 e^{-(a+b)t} + C_1, \tag{4.6}$$

$$\langle x^2(t) \rangle = A_2(t) e^{(b-a)t} + B_2(t) e^{-(a+b)t} + C_2, \tag{4.7}$$

so the variance is

$$\sigma_x^2(t) = A(t)e^{(b-a)t} + B(t)e^{-(a+b)t} + C(t). \tag{4.8}$$

In these equations, $a = (\kappa + k_1 + k_2)/2$ and $b = \sqrt{a^2 - \kappa k_2}$ are effective rates having dimensions of inverse time, while the A, B, and C factors are provided in table 4.1.

Table 4.1: Abbreviations used in the expressions of the mean (4.6), second moment (4.7) and variance (4.8) of bedload tracers.

$A_1 = \frac{v}{2b}\left[\theta_2 + \frac{k_1 + \theta_2\kappa}{b-a}\right]$
$B_1 = -\frac{v}{2b}\left[\theta_2 - \frac{k_1 + \theta_2\kappa}{a+b}\right]$
$C_1 = -\frac{v}{2b}\left[\frac{k_1 + \theta_2\kappa}{b-a} + \frac{k_1 + \theta_2\kappa}{a+b}\right]$
$A_2(t) = \frac{v^2}{2b^3}\left[(bt-1)[k_1 + \theta_2(2\kappa + k_1 + b - a)] + \theta_2 b + \frac{(\kappa + k_1)(\theta_2\kappa + k_1)}{(b-a)^2}[(bt-1)(b-a) - b]\right]$
$B_2(t) = \frac{v^2}{2b^3}\left[(bt+1)[k_1 + \theta_2(2\kappa + k_1 - a - b)] + \theta_2 b - \frac{(\kappa + k_1)(\theta_2\kappa + k_1)}{(a+b)^2}[(bt+1)(a+b) + b]\right]$
$C_2 = \frac{v^2}{2b^3}(\kappa + k_1)(\theta_2\kappa + k_1)\left[\frac{2b-a}{(b-a)^2} + \frac{a+2b}{(a+b)^2}\right]$
$A(t) = A_2(t) - 2A_1C_1 - A_1^2\exp[(b-a)t]$
$B(t) = B_2(t) - 2B_1C_1 - B_1^2\exp[-(a+b)t]$
$C(t) = C_2 - C_1^2 - 2A_1B_1\exp[-2at]$

The positional variance (4.8) is plotted in figure 4.2 for conditions $\theta_1 = 1$ and $k_2 \gg k_1 \gg \kappa$. We interpret "$\gg$" to mean "of at least an order of magnitude greater". These conditions are most relevant to tracers in gravel-bed rivers, since they represent that grains are initially at rest (*Hassan et al.*, 1991; *Wu et al.*, 2019a), motions are typically much shorter than rests (*Einstein*, 1937; *Hubbell and Sayre*, 1964), and burial requires a much longer time than typical rests (*Ferguson and Hoey*, 2002; *Haschenburger*, 2013; *Hassan and Church*, 1994). Figure 4.2 demonstrates that under these conditions the variance (4.8) shows three diffusion ranges with approximate power law scaling ($\sigma_x^2 \propto t^\gamma$) that we identify as the local, intermediate, and global ranges proposed by Nikora et al., followed by a fourth range of no diffusion ($\sigma_x^2 = \text{const}$) stemming from the burial of all tracers. We suggest to call the

fourth range geomorphic, since any further transport in this range can occur only if scour re-exposes buried grains to the flow (*Martin et al.*, 2014; *Voepel et al.*, 2013; *Wu et al.*, 2019b; **?**).

4.1.5 Diffusion exponents

Two limiting cases of equation (4.8) provide the scaling exponents γ of the diffusion $\sigma_x^2 \propto t^\gamma$ in each range. Limit (1) represents times so short a negligible amount of sediment burial has occurred, $t \ll 1/\kappa$, while limit (2) represents times so long motion intervals appear as instantaneous steps of mean length $l = v/k_2$, $1/k_2 \to 0$ while $v/k_2 =$ constant. Limit (1) provides local exponent $2 \leq \gamma \leq 3$ depending on the initial conditions θ_i, and intermediate exponent $\gamma = 1$. If grains start in motion or rest exclusively, meaning one $\theta_i = 0$, the local exponent is $\gamma = 3$, while if grains start in a mixture of motion and rest states, meaning neither θ_i is zero, the local exponent is $\gamma = 2$. Limit (2) provides global exponent $1 \leq \gamma \leq 3$ depending on the relative importance of κ and k_1. In the extreme $k_1/\kappa \ll 1$, we find $\gamma = 1$ in the global range, while in the opposite extreme $k_1/\kappa \to \infty$ we find $\gamma = 3$. We summarize when $k_2 \gg k_1 \gg \kappa$ so all three diffusion ranges exist, equation (4.8) implies:

1. local range super-diffusion with $2 < \gamma < 3$ depending on whether grains start from purely motion or rest ($\gamma = 3$) or from a mixture of both states ($\gamma = 2$),

2. intermediate range normal diffusion $\gamma = 1$ independent of model parameters, and

3. global range super-diffusion $1 < \gamma < 3$ depending on whether burial happens relatively slowly ($\gamma \to 1$) or quickly ($\gamma \to 3$) compared to surface resting times.

Finally, the burial of all tracers generates a geomorphic range of no diffusion.

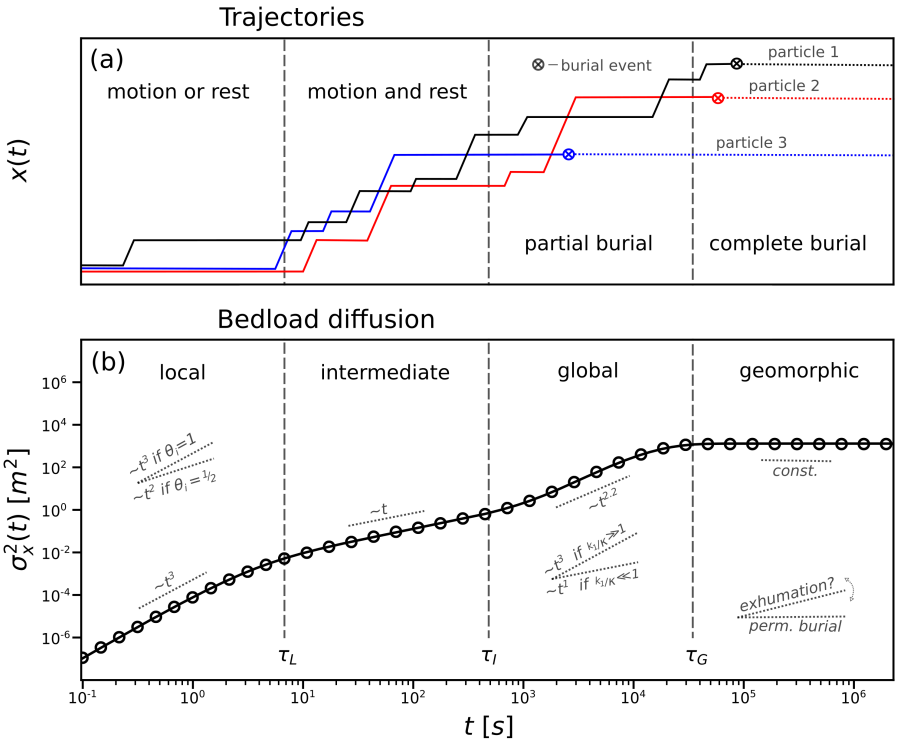

Figure 4.2: Panel (a) sketches conceptual trajectories of three grains, while panel (b) depicts the variance (4.8) with mean motion time 1.5 s, resting time 30.0 s, and movement velocity 0.1 m/s – values comparable to laboratory experiments transporting small (5 mm) gravels (*Lajeunesse et al.*, 2010; *Martin et al.*, 2012). The burial timescale is 7200.0s (two hours), and grains start from rest ($\theta_1 = 1$). The solid line is equation (4.8), and the points are numerically simulated. Panel (b) demonstrates four distinct scaling ranges of σ_x^2: local, intermediate, global, and geomorphic. The first three are diffusive. Three crossover times τ_L, τ_I, and τ_G divide the ranges. Within each range, a slope key demonstrates the scaling $\sigma_x^2 \propto t^\gamma$. Panel (a) demonstrates that different mixtures of motion, rest, and burial states generate the ranges. At local timescales, grains usually either rest or move; at intermediate timescales, they transition between rest and motion; at global timescales, they transition between rest, motion, and burial; and at geomorphic timescales, all grains bury. Additional slope keys in the local and global ranges of panel (b) illustrate the effect of initial conditions and rest/burial timescales on the diffusion, while the additional slope key within the geomorphic range demonstrates the expected scaling when burial is not permanent, as we discuss in section 4.2.

4.2 Discussion

4.2.1 Local and intermediate ranges with comparison to earlier work

We extended *Einstein* (1937) by including motion and burial processes in a multi-state random walk (*Weeks and Swinney*, 1998; *Weiss*, 1994) to demonstrate that a group of bedload tracers moving downstream while gradually becoming buried will generate a super-diffusive local range (*Fathel et al.*, 2016; *Martin et al.*, 2012; *Witz et al.*, 2019), a normal-diffusive intermediate range (*Nakagawa and Tsujimoto 9 Kyoto*, 1977; *Yano*, 1969), and a super-diffusive global range (*Bradley*, 2017; *Bradley et al.*, 2010), before the diffusion eventually terminates in a geomorphic range (*Hassan and Bradley*, 2017). *Nikora et al.* (2002) highlighted the need for such a physical description, although they suggested to use a two-state random walk between motion and rest states with heavy-tailed resting times, and they did not discuss sediment burial. However, other works have demonstrated that a two-state walk with heavy-tailed rests provides two diffusion ranges – not three (*Fowler*, 2016; *Weeks et al.*, 1996), and although heavy-tailed resting times have been documented for surface particles (*Fraccarollo and Hassan*, 2019; *Liu et al.*, 2019), they are more often associated with buried particles (*Martin et al.*, 2012, 2014; *Olinde and Johnson*, 2015; *Shi and Wang*, 2014; *Voepel et al.*, 2013; **?**), while surface particles retain light-tailed resting times (*Ancey et al.*, 2006; *Einstein*, 1937; *Nakagawa and Tsujimoto 9 Kyoto*, 1977; *Yano*, 1969). Accordingly, we developed a random walk model of bedload trajectories with light-tailed surface resting times that incorporates sediment burial.

The local and intermediate range diffusion characteristics resulting from our model correspond closely to the original Nikora et al. concepts, while our global range has a different origin than Nikora et al. envisioned. *Nikora et al.* (2001) explained that local diffusion results from the non-fractal (smooth) characteristics of bedload trajectories between subsequent interactions with the bed, while intermediate diffusion results from the fractal (rough) characteristics of bedload trajectories after many interactions with the bed. Our model represents these conclusions: non-fractal (and super-diffusive) bedload trajectories exist on timescales short enough that each grain is either resting or moving, while fractal (and normal-

diffusive) bedload trajectories exist on timescales when grains are actively switching between motion and rest states. We conclude that local and intermediate ranges stem from the interplay between motion and rest timescales, as demonstrated by earlier two-state random walk models (*Lajeunesse et al.*, 2018; *Lisle et al.*, 1998) and by all Newtonian models that develop sequences of motions and rests (*Bialik et al.*, 2012; *Nikora et al.*, 2001), even those including heavy-tailed rests (*Fowler*, 2016).

4.2.2 Global and geomorphic ranges with next steps for research

Nikora et al. explained that divergent resting times generate a sub-diffusive global range. However, studies have demonstrated that divergent resting times can generate super-diffusion in asymmetric random walks (*Weeks and Swinney*, 1998; *Weeks et al.*, 1996), and both experiments (*Bradley*, 2017; *Bradley et al.*, 2010) and models (*Shi and Wang*, 2014; *Wu et al.*, 2019a,b) of bedload tracers undergoing burial have demonstrated global range super-diffusion. While our results also show global range super-diffusion, they do not necessarily refute the Nikora et al. conclusion of sub-diffusion at long timescales. We assumed sediment burial was a permanent condition which developed a non-diffusive geomorphic range. In actuality, burial is a temporary condition, because bed scour can exhume buried sediment back into transport (*Wu et al.*, 2019b), probably after heavy-tailed intervals (*Martin et al.*, 2014; *Voepel et al.*, 2013; **?**). We anticipate that a generalization of our model to include heavy-tailed timescales between burial and exhumation would develop four ranges of diffusion, where the long-time decay of the exhumation time distribution would dictate the geomorphic range diffusion characteristics as depicted in figure 4.2. If cumulative exhumation times decay faster than $T^{-1/2}$, as suggested by equilibrium transport models (*Martin et al.*, 2014; *Voepel et al.*, 2013; **?**) and laboratory experiments (*Martin et al.*, 2012, 2014), we expect a super-diffusive geomorphic range (*Weeks and Swinney*, 1998). However, if they decay slower than $T^{-1/2}$, as implicitly suggested by the data of *Olinde and Johnson* (2015), we expect a genuinely sub-diffusive geomorphic range (*Weeks and Swinney*, 1998), leaving Nikora et al. with the final word on long-time sub-diffusion.

The analytical solution of bedload diffusion in equation (4.8) reduces exactly to

the analytical solutions of the *Lisle et al.* (1998) and *Lajeunesse et al.* (2018) models in the limit without burial ($\kappa \to 0$), the *Wu et al.* (2019a) model in the limit of instantaneous steps ($k_2 \to \infty$ and $l = v/k_2$), and the original *Einstein* (1937) model in the limit of instantaneous steps without burial. These reductions demonstrate that the majority of recent bedload diffusion models, whether developed from Exner-type equations (*Pelosi and Parker*, 2014; *Shi and Wang*, 2014; *Wu et al.*, 2019a) or advection-diffusion equations (*Lajeunesse et al.*, 2018; *Lisle et al.*, 1998), can be viewed equivalently as continuous-time random walks applied to individual bedload trajectories. Within random walk theory, sophisticated descriptions of transport with variable velocities (*Masoliver and Weiss*, 1994; *Zaburdaev et al.*, 2008), correlated motions (*Escaff et al.*, 2018; *Vicsek and Zafeiris*, 2012), and anomalous diffusion (*Fa*, 2014; *Masoliver*, 2016; *Metzler et al.*, 2014) have been developed. Meanwhile, in bedload transport research, variable velocities (*Furbish et al.*, 2012a; *Heyman et al.*, 2016; *Lajeunesse et al.*, 2010), correlated motions (*Heyman et al.*, 2014; *Lee and Jerolmack*, 2018; *Saletti and Hassan*, 2020), and anomalous diffusion (*Bradley*, 2017; *Fathel et al.*, 2016; *Schumer et al.*, 2009) constitute open research issues. We believe further developing the linkage between existing bedload models and random walk concepts could rapidly progress our understanding.

4.3 Conclusion

We developed a random walk model to describe sediment tracers transporting through a river channel as they gradually become buried, providing a physical description of the local, intermediate, and global diffusion ranges identified by *Nikora et al.* (2002). Pushing their ideas somewhat further, we proposed a geomorphic range to describe diffusion characteristics at timescales larger than the global range when burial and exhumation both moderate downstream transport. At base level, our model demonstrates that (1) durations of sediment motions, (2) durations of sediment rest, and (3) the sediment burial process are sufficient to develop three diffusion ranges that terminate when all tracers become buried. A next step is to incorporate exhumation to better understand the geomorphic range. Ultimately, we emphasize that the multi-state random walk formalism used in this paper implicitly underlies most existing bedload diffusion models and provides a powerful tool for

researchers targeting landscape-scale understanding from statistical concepts of the underlying grain-scale dynamics.

Chapter 5

Summary and future work

Bibliography

Aberle, J., and V. Nikora, Statistical properties of armored gravel bed surfaces, *Water Resources Research*, *42*, 1–11, 2006. → pages 28, 31

Amir, M., V. I. Nikora, and M. T. Stewart, Pressure forces on sediment particles in turbulent open-channel flow: A laboratory study, *Journal of Fluid Mechanics*, *757*, 458–497, 2014. → page 30

Ancey, C., T. Böhm, M. Jodeau, and P. Frey, Statistical description of sediment transport experiments, *Physical Review E - Statistical, Nonlinear, and Soft Matter Physics*, *74*, 1–14, 2006. → pages 11, 13, 25, 36, 43

Ancey, C., A. C. Davison, T. Böhm, M. Jodeau, and P. Frey, Entrainment and motion of coarse particles in a shallow water stream down a steep slope, *Journal of Fluid Mechanics*, *595*, 83–114, 2008. → pages ix, xi, 3, 11, 13, 14, 16, 17, 18, 19, 20, 23, 24, 25, 28, 29

Ancey, C., P. Bohorquez, and J. Heyman, Stochastic interpretation of the advection-diffusion, *Journal of Geophysical Research : Earth Surface*, *120*, 325–345, 2015. → page 30

Arfken, G., *Mathematical methods for physicists*, Academic Press, Inc., 1985. → page 38

Barik, D., P. K. Ghosh, and D. S. Ray, Langevin dynamics with dichotomous noise; Direct simulation and applications, *Journal of Statistical Mechanics: Theory and Experiment*, 2006. → page 38

Bennett, C. H., Serially deposited amorphous aggregates of hard spheres, *Journal of Applied Physics*, *43*, 2727–2734, 1972. → pages 14, 18

Bialik, R. J., V. I. Nikora, and P. M. Rowiński, 3D Lagrangian modelling of saltating particles diffusion in turbulent water flow, *Acta Geophysica*, *60*, 1639–1660, 2012. → pages 34, 35, 44

Bialik, R. J., V. I. Nikora, M. Karpiński, and P. M. Rowiński, Diffusion of bedload particles in open-channel flows: distribution of travel times and second-order statistics of particle trajectories, *Environmental Fluid Mechanics*, *15*, 1281–1292, 2015. → page 34

Bradley, D. N., Direct Observation of Heavy-Tailed Storage Times of Bed Load Tracer Particles Causing Anomalous Superdiffusion, *Geophysical Research Letters*, *44*, 12,227–12,235, 2017. → pages 12, 30, 34, 43, 44, 45

Bradley, D. N., G. E. Tucker, and D. A. Benson, Fractional dispersion in a sand bed river, *Journal of Geophysical Research*, *115*, F00A09, 2010. → pages 43, 44

Celik, A. O., P. Diplas, C. L. Dancey, and M. Valyrakis, Impulse and particle dislodgement under turbulent flow conditions, *Physics of Fluids*, *22*, 1–13, 2010. → page 11

Charru, F., H. Mouilleron, and O. Eiff, Erosion and deposition of particles on a bed sheared by a viscous flow, *Journal of Fluid Mechanics*, *519*, 55–80, 2004. → pages 2, 14, 30

Correa, A., D. Windhorst, D. Tetzlaff, P. Crespo, R. Célleri, J. Feyen, and L. Breuer, Accelerating advances in continental domain hydrologic modeling, *Water Resources Research*, *53*, 5998–6017, 2017. → page 16

Dhont, B., and C. Ancey, Are Bedload Transport Pulses in Gravel Bed Rivers Created by Bar Migration or Sediment Waves?, *Geophysical Research Letters*, *45*, 5501–5508, 2018. → pages 13, 28

Dwivedi, A., B. W. Melville, A. Y. Shamseldin, and T. K. Guha, Analysis of hydrodynamic lift on a bed sediment particle, *Journal of Geophysical Research: Earth Surface*, *116*, 2011. → page 11

Einstein, H. A., Bed load transport as a probability problem, Ph.D. thesis, ETH Zurich, 1937. → pages xiii, 2, 11, 12, 28, 33, 34, 35, 36, 38, 39, 40, 43, 45

Einstein, H. A., *The bedload function for sediment transportation in open channel flows*, technical ed., Soil Conservation Service, Washington, DC, 1950. → pages 3, 11, 13, 14, 28

Escaff, D., R. Toral, C. Van Den Broeck, and K. Lindenberg, A continuous-time persistent random walk model for flocking, *Chaos*, *28*, 1–11, 2018. → page 45

Fa, K. S., Uncoupled continuous-time random walk model: Analytical and numerical solutions, *Physical Review E - Statistical, Nonlinear, and Soft Matter Physics*, *89*, 1–9, 2014. → page 45

Fathel, S., D. Furbish, and M. Schmeeckle, Parsing anomalous versus normal diffusive behavior of bedload sediment particles, *Earth Surface Processes and Landforms*, *41*, 1797–1803, 2016. → pages 34, 43, 45

Fathel, S. L., D. J. Furbish, and M. W. Schmeeckle, Experimental evidence of statistical ensemble behavior in bed load sediment transport, *Journal of Geophysical Research F: Earth Surface*, *120*, 2298–2317, 2015. → pages 2, 13, 31, 36

Ferguson, R. I., and T. B. Hoey, Long-term slowdown of river tracer pebbles: Generic models and implications for interpreting short-term tracer studies, *Water Resources Research*, *38*, 17–1–17–11, 2002. → page 40

Ferguson, R. I., D. J. Bloomer, T. B. Hoey, and A. Werritty, Mobility of river tracer pebbles over different timescales, *Water Resources Research*, *38*, 3–1–3–8, 2002. → page 34

Fowler, K. J. A., Simulating runoff under changing climatic conditions, *Water Resources Research*, *52*, 1–24, 2016. → pages 34, 43, 44

Fraccarollo, L., and M. A. Hassan, Einstein conjecture and resting-Time statisticsÂ inÂ the bed-load transport of monodispersedÂ particles, *Journal of Fluid Mechanics*, *876*, 1077–1089, 2019. → page 43

Furbish, D. J., A. E. Ball, and M. W. Schmeeckle, A probabilistic description of the bed load sediment flux: 4. Fickian diffusion at low transport rates, *Journal of Geophysical Research: Earth Surface*, *117*, 1–13, 2012a. → pages 3, 34, 45

Furbish, D. J., P. K. Haff, J. C. Roseberry, and M. W. Schmeeckle, A probabilistic description of the bed load sediment flux: 1. Theory, *Journal of Geophysical Research: Earth Surface*, *117*, 2012b. → pages 11, 13, 14

Furbish, D. J., S. L. Fathel, and M. W. Schmeeckle, Particle motions and bedload theory: The entrainment forms of the flux and the exner equation, in *Gravel-Bed Rivers: Process and Disasters*, edited by D. Tsutsumi and J. B. Laronne, 1 ed., chap. 4, pp. 97–120, John Wiley & Sons Ltd., 2017. → pages 13, 34

Gaeuman, D., R. Stewart, B. Schmandt, and C. Pryor, Geomorphic response to gravel augmentation and high-flow dam release in the Trinity River, California, *Earth Surface Processes and Landforms*, *42*, 2523–2540, 2017. → pages 11, 33

Gardiner, C. W., *Handbook of stochastic methods for physics, chemistry and the natural sciences*, Springer-Verlag, 1983. → pages 5, 17, 20, 30

Gillespie, D. T., Exact stochastic simulation of coupled chemical reactions, *Journal of Physical Chemistry*, *81*, 2340–2361, 1977. → page 17

Gillespie, D. T., Stochastic simulation of chemical kinetics, *Annual Review of Physical Chemistry*, *58*, 35–55, 2007. → pages 16, 17, 18

González, C., D. H. Richter, D. Bolster, S. Bateman, J. Calantoni, and C. Escauriaza, Characterization of bedload intermittency near the threshold of motion using a Lagrangian sediment transport model, *Environmental Fluid Mechanics*, *17*, 111–137, 2017. → page 11

Gordon, R., J. B. Carmichael, and F. J. Isackson, Saltation of plastic balls in a 'one-dimensional' flume, *Water Resources Research*, *8*, 444–459, 1972. → pages 2, 35

Haschenburger, J. K., Tracing river gravels: Insights into dispersion from a long-term field experiment, *Geomorphology*, *200*, 121–131, 2013. → pages 34, 40

Hassan, M. A. ., and D. N. Bradley, Geomorphic controls on tracer particle dispersion in gravel-bed rivers, in *Gravel-Bed Rivers: Process and Disasters*, edited by D. Tsutsumi and J. B. Laronne, 1st ed., pp. 159–184, John Wiley & Sons Ltd., 2017. → pages 11, 33, 34, 43

Hassan, M. A., and M. Church, Vertical mixing of coarse particles in gravel bed rivers: A kinematic model, *Water Resources Research*, *30*, 1173–1185, 1994. → page 40

Hassan, M. A., M. Church, and A. P. Schick, Distance of movement of coarse particles in gravel bed streams, *Water Resources Research*, *27*, 503–511, 1991. → pages 28, 34, 35, 40

Hassan, M. A., B. J. Smith, D. L. Hogan, D. S. Luzi, A. E. Zimmermann, and B. C. Eaton, 18 Sediment storage and transport in coarse bed streams: scale considerations, in *Developments in Earth Surface Processes*, edited by H. Habersack, H. Piegay, and M. Rinaldi, vol. 11, chap. 18, pp. 473–496, Elsevier B.V, 2007. → page 30

Hassan, M. A., H. Voepel, R. Schumer, G. Parker, and L. Fraccarollo, Displacement characteristics of coarse fluvial bed sediment, *Journal of Geophysical Research: Earth Surface*, *118*, 155–165, 2013. → page 34

Heyman, J., A study of the spatio-temporal behaviour of bed load transport rate fluctuations, *PhD Dissertation*, *6256*, 116, 2014. → page 13

Heyman, J., F. Mettra, H. B. Ma, and C. Ancey, Statistics of bedload transport over steep slopes: Separation of time scales and collective motion, *Geophysical Research Letters*, *40*, 128–133, 2013. → page 13

Heyman, J., H. B. Ma, F. Mettra, and C. Ancey, Spatial correlations in bed load transport : Evidence, importance, and modeling, *Journal of Geophysical Research: Earth Surface*, *119*, 1751–1767, 2014. → pages 13, 30, 45

Heyman, J., P. Bohorquez, and C. Ancey, Entrainment, motion, and deposition of coarse particles transported by water over a sloping mobile bed, *Journal of Geophysical Research: Earth Surface*, *121*, 1931–1952, 2016. → pages 2, 13, 28, 31, 45

Hubbell, D., and W. Sayre, Sand Transport Studies with Radioactive Tracers, *Journal of the Hydraulics Division*, *90*, 39–68, 1964. → pages 11, 12, 28, 35, 40

Kraichnan, R. H., Diffusion by a random velocity field, *Physics of Fluids*, *13*, 22–31, 1970. → page 34

Lajeunesse, E., L. Malverti, and F. Charru, Bed load transport in turbulent flow at the grain scale: Experiments and modeling, *Journal of Geophysical Research: Earth Surface*, *115*, 2010. → pages xiv, 31, 42, 45

Lajeunesse, E., O. Devauchelle, and F. James, Advection and dispersion of bed load tracers, *Earth Surface Dynamics*, *6*, 389–399, 2018. → pages 3, 5, 11, 44, 45

Lee, D. B., and D. Jerolmack, Determining the scales of collective entrainment in collision-driven bed load, *Earth Surface Dynamics*, *6*, 1089–1099, 2018. → pages 13, 29, 45

Lisle, I. G., C. W. Rose, W. L. Hogarth, P. B. Hairsine, G. C. Sander, and J. Y. Parlange, Stochastic sediment transport in soil erosion, *Journal of Hydrology*, *204*, 217–230, 1998. → pages xiii, 3, 5, 35, 36, 38, 39, 44, 45

Liu, M. X., A. Pelosi, and M. Guala, A Statistical Description of Particle Motion and Rest Regimes in Open-Channel Flows Under Low Bedload Transport, *Journal of Geophysical Research: Earth Surface*, *124*, 2666–2688, 2019. → pages 12, 31, 43

Ma, H., J. Heyman, X. Fu, F. Mettra, C. Ancey, and G. Parker, Bed load transport over a broad range of timescales: Determination of three regimes of fluctuations, *Journal of Geophysical Research: Earth Surface*, *119*, 2653–2673, 2014. → page 13

Macklin, M. G., P. A. Brewer, K. A. Hudson-Edwards, G. Bird, T. J. Coulthard, I. A. Dennis, P. J. Lechler, J. R. Miller, and J. N. Turner, A geomorphological approach to the management of rivers contaminated by metal mining, *Geomorphology*, *79*, 423–447, 2006. → pages 11, 33

Malmon, D. V., S. L. Reneau, T. Dunne, D. Katzman, and P. G. Drakos, Influence of sediment storage on downstream delivery of contaminated sediment, *Water Resources Research*, *41*, 1–17, 2005. → page 11

Marcum, J. I., A Statistical Theory of Target Detection By Pulsed Radar, *IRE Transactions on Information Theory*, *6*, 59–267, 1960. → page 38

Martin, R. L., D. J. Jerolmack, and R. Schumer, The physical basis for anomalous diffusion in bed load transport, *Journal of Geophysical Research: Earth Surface*, *117*, 1–18, 2012. → pages xiv, 11, 12, 34, 36, 42, 43, 44

Martin, R. L., P. K. Purohit, and D. J. Jerolmack, Sedimentary bed evolution as a mean-reverting random walk: Implications for tracer statistics, *Geophysical Research Letters*, *41*, 6152–6159, 2014. → pages 12, 16, 18, 20, 26, 27, 28, 29, 30, 31, 34, 41, 43, 44

Masoliver, J., Fractional telegrapher's equation from fractional persistent random walks, *Physical Review E*, *93*, 1–10, 2016. → page 45

Masoliver, J., and G. H. Weiss, Telegrapher's equations with variable propagation speeds, *Physical Review E*, *49*, 3852–3854, 1994. → page 45

Metzler, R., and J. Klafter, The random walk's guide to anomalous diffusion: A fractional dynamics approach, *Physics Report*, *339*, 1–77, 2000. → pages 33, 38

Metzler, R., J. H. Jeon, A. G. Cherstvy, and E. Barkai, Anomalous diffusion models and their properties: Non-stationarity, non-ergodicity, and ageing at the

centenary of single particle tracking, *Physical Chemistry Chemical Physics*, *16*, 24,128–24,164, 2014. → page 45

Montroll, E. W., Random walks on lattices, *Journal of Mathematical Physics*, *6*, 193–220, 1964. → pages 2, 35

Nakagawa, H., and T. Tsujimoto 9 Kyoto, On probabilistic characteristics of motion of individual sediment particles on stream beds., in *Hydraulic Problems Solved by Stochastic Methods: Second International IAHR Symposium on Stochastic Hydraulics*, pp. 293–320, Water Resources Publications, Lund, Sweden, 1977. → pages 11, 12, 28, 34, 35, 43

Nelson, P. A., D. Bellugi, and W. E. Dietrich, Delineation of river bed-surface patches by clustering high-resolution spatial grain size data, *Geomorphology*, *205*, 102–119, 2014. → page 30

Newman, M. E., Power laws, Pareto distributions and Zipf's law, *Contemporary Physics*, *46*, 323–351, 2005. → page 27

Nikora, V., J. Heald, D. Goring, and I. McEwan, Diffusion of saltating particles in unidirectional water flow over a rough granular bed, *Journal of Physics A: Mathematical and General*, *34*, 2001. → pages 33, 34, 43, 44

Nikora, V., H. Habersack, T. Huber, and I. McEwan, On bed particle diffusion in gravel bed flows under weak bed load transport, *Water Resources Research*, *38*, 17–1–17–9, 2002. → pages 33, 34, 35, 43, 45

Olinde, L., and J. P. L. Johnson, Using RFID and accelerometer-embedded tracers to measure probabilities of bed load transport, step lengths, and rest times in a mountain stream, *Water Resources Research*, *51*, 7525–7589, 2015. → pages 12, 30, 43, 44

Paintal, A. S., A stochastic model of bed load transport, *Journal of Hydraulic Research*, *9*, 527–554, 1971. → pages 11, 15, 35

Papangelakis, E., and M. A. Hassan, The role of channel morphology on the mobility and dispersion of bed sediment in a small gravel-bed stream, *Earth Surface Processes and Landforms*, *41*, 2191–2206, 2016. → page 34

Pelosi, A., and G. Parker, Morphodynamics of river bed variation with variable bedload step length, *Earth Surface Dynamics*, *2*, 243–253, 2014. → page 45

Pender, G., T. B. Hoey, C. Fuller, and I. K. McEwan, Selective bedload transport during the degradation of a well sorted graded sediment bed, *Journal of Hydraulic Research*, *39*, 269–277, 2001. → page 16

Philip, J. R., Diffusion by continuous movements, *Physics of Fluids*, *11*, 38–42, 1968. → page 33

Phillips, C. B., R. L. Martin, and D. J. Jerolmack, Impulse framework for unsteady flows reveals superdiffusive bed load transport, *Geophysical Research Letters*, *40*, 1328–1333, 2013. → page 34

Pielou, E. C., *Mathematical Ecology*, 1 ed., John Wiley & Sons Ltd., New York, NY, 2008. → page 17

Prudnikov, A. P., Y. A. Brychkov, O. I. Marichev, and R. H. Romer, *Integrals and Series*, Gordon and Breach, New York, 1988. → page 38

Redner, S., and J. R. Dorfman, *A Guide to First-Passage Processes*, vol. 70, Cambridge University Press, Cambridge, 2002. → pages 12, 26

Roseberry, J. C., M. W. Schmeeckle, and D. J. Furbish, A probabilistic description of the bed load sediment flux: 2. Particle activity and motions, *Journal of Geophysical Research: Earth Surface*, *117*, 2012. → pages 13, 31, 36

Saletti, M., and M. A. Hassan, Width variations control the development of grain structuring in steep step-pool dominated streams: insight from flume experiments, *Earth Surface Processes and Landforms*, *45*, 1430–1440, 2020. → page 45

Schmeeckle, M. W., J. M. Nelson, and R. L. Shreve, Forces on stationary particles in near-bed turbulent flows, *Journal of Geophysical Research: Earth Surface*, *112*, 1–21, 2007. → page 11

Schmidt, M. G., F. Sagués, and I. M. Sokolov, Mesoscopic description of reactions for anomalous diffusion: A case study, *Journal of Physics Condensed Matter*, *19*, 2007. → page 36

Schumer, R., M. M. Meerschaert, and B. Baeumer, Fractional advection-dispersion equations for modeling transport at the Earth surface, *Journal of Geophysical Research: Earth Surface*, *114*, 1–15, 2009. → pages 38, 45

Sekine, M., and H. Kikkawa, Mechanics of saltating grains. II, *Journal of Hydraulic Engineering*, *118*, 536–558, 1992. → page 34

Shi, Z., and G. Wang, Hydrological response to multiple large distant earthquakes in the Mile well, China, *Journal of Geophysical Research F: Earth Surface*, *119*, 2448–2459, 2014. → pages 28, 43, 44, 45

Shih, W. R., P. Diplas, A. O. Celik, and C. Dancey, Accounting for the role of turbulent flow on particle dislodgement via a coupled quadrant analysis of velocity and pressure sequences, *Advances in Water Resources*, *101*, 37–48, 2017. → page 30

Shlesinger, M. F., Asymptotic solutions of continuous-time random walks, *Journal of Statistical Physics*, *10*, 421–434, 1974. → page 39

Singh, A., K. Fienberg, D. J. Jerolmack, J. Marr, and E. Foufoula-Georgiou, Experimental evidence for statistical scaling and intermittency in sediment transport rates, *Journal of Geophysical Research: Earth Surface*, *114*, 1–16, 2009. → pages 3, 13, 18, 31

Singh, A., E. Foufoula-Georgiou, F. Porté-Agel, and P. R. Wilcock, Coupled dynamics of the co-evolution of gravel bed topography, flow turbulence and sediment transport in an experimental channel, *Journal of Geophysical Research F: Earth Surface*, *117*, 1–20, 2012. → pages 13, 28, 31

Sokolov, I. M., Models of anomalous diffusion in crowded environments, *Soft Matter*, *8*, 9043–9052, 2012. → page 33

Swift, R. J., A Stochastic Predator-Prey Model, *Bulletin of the Irish Mathematical Society*, *48*, 57–63, 2002. → page 17

Temme, N. M., and D. Zwillinger, *Special Functions: An Introduction to the Classical Functions of Mathematical Physics*, vol. 65, John Wiley & Sons Ltd., 1997. → page 38

Vicsek, T., and A. Zafeiris, Collective motion, *Physics Reports*, *517*, 71–140, 2012. → page 45

Voepel, H., R. Schumer, and M. A. Hassan, Sediment residence time distributions: Theory and application from bed elevation measurements, *Journal of Geophysical Research: Earth Surface*, *118*, 2557–2567, 2013. → pages 12, 26, 27, 28, 30, 34, 41, 43, 44

Vowinckel, B., T. Kempe, and J. Fröhlich, Fluid-particle interaction in turbulent open channel flow with fully-resolved mobile beds, *Advances in Water Resources*, *72*, 32–44, 2014. → page 11

Weeks, E. R., and H. L. Swinney, Anomalous diffusion resulting from strongly asymmetric random walks, *Physical Review E - Statistical Physics, Plasmas, Fluids, and Related Interdisciplinary Topics*, *57*, 4915–4920, 1998. → pages 12, 36, 37, 38, 39, 43, 44

Weeks, E. R., J. S. Urbach, and H. L. Swinney, Anomalous diffusion in asymmetric random walks with a quasi-geostrophic flow example, *Physica D: Nonlinear Phenomena*, *97*, 291–310, 1996. → pages 43, 44

Weiss, G. H., The two-state random walk, *Journal of Statistical Physics*, *15*, 157–165, 1976. → page 35

Weiss, G. H., *Aspects and Applications of the Random Walk.*, North Holland, Amsterdam, 1994. → pages 35, 36, 37, 43

Wiberg, P. L., and J. D. Smith, A theoretical model for saltating grains in water., *Journal of Geophysical Research*, *90*, 7341–7354, 1985. → page 11

Witz, M. J., S. Cameron, and V. Nikora, Bed particle dynamics at entrainment, *Journal of Hydraulic Research*, *57*, 464–474, 2019. → page 43

Wong, M., G. Parker, P. DeVries, T. M. Brown, and S. J. Burges, Experiments on dispersion of tracer stones under lower-regime plane-bed equilibrium bed load transport, *Water Resources Research*, *43*, 1–23, 2007. → pages 12, 13, 15, 16, 18, 28

Wu, Z., E. Foufoula-Georgiou, G. Parker, A. Singh, X. Fu, and G. Wang, Analytical Solution for Anomalous Diffusion of Bedload Tracers Gradually Undergoing Burial, *Journal of Geophysical Research: Earth Surface*, *124*, 21–37, 2019a. → pages 11, 28, 35, 36, 40, 44, 45

Wu, Z., A. Singh, X. Fu, and G. Wang, Transient Anomalous Diffusion and Advective Slowdown of Bedload Tracers by Particle Burial and Exhumation, *Water Resources Research*, *55*, 7964–7982, 2019b. → pages 28, 41, 44

Yang, C. T., and W. Sayre, Stochastic Model for Sand Dispersion, *Journal of the Hydraulics Division*, *97*, 265–288, 1971. → pages 27, 28, 35

Yano, K., Tracer Studies on the Movement of Sand and Gravel, in *Proceedings of the 12th Congress IAHR, Vol 2.*, pp. 121–129, Kyoto, Japan, 1969. → pages 12, 34, 35, 43

Zaburdaev, V., M. Schmiedeberg, and H. Stark, Random walks with random velocities, *Physical Review E - Statistical, Nonlinear, and Soft Matter Physics*, *78*, 1–5, 2008. → page 45

Zhang, Y., M. M. Meerschaert, and A. I. Packman, Linking fluvial bed sediment transport across scales, *Geophysical Research Letters*, *39*, 1–6, 2012. → page 34